KIM, Jang Ho, 1932-

A STUDY OF VAPORS OF PURE BISMUTH AND LEAD. . . .SOME THERMODYNAMIC PROPERTIES OF THE SILVER-BISMUTH LIQUID ALLOYS.

The University of Oklahoma, Ph.D., 1966
Engineering, metallurgy

University Microfilms, Inc., Ann Arbor, Michigan

THE UNIVERSITY OF OKLAHOMA

GRADUATE COLLEGE

A STUDY OF VAPORS OF PURE BISMUTH AND LEAD. . . . SOME THERMODYNAMIC PROPERTIES OF THE SILVER-BISMUTH LIQUID ALLOYS

A DISSERTATION

SUBMITTED TO THE GRADUATE FACULTY

in partial fulfillment of the requirements
for the degree of

DOCTOR OF PHILOSOPHY

BY

JANG HO KIM

1966

A STUDY OF VAPORS OF PURE LIQUID BISMUTH AND LEAD. . . .

SOME THERMODYNAMIC PROPERTIES OF

SILVER-BISMUTH LIQUID ALLOYS

APPROVED BY

DISSERTATION COMMITTEE

ACKNOWLEDGEMENT

The author expresses his sincere appreciation to Professor Andrew Cosgarea, Jr. for his interest, liberal contribution of time and valuable suggestions; to Professor Raymond Dewitt Daniels and Professor Frank Ballew Canfield, for their contributions.

The author is indebted to Professor Albert E. Wilson for his guidance and his contribution of time in developing the automatic recording and controlling microbalance system and also to Professor Sherril D. Christian for his discussion and his guidance in constructing the quartz microbalance.

The author acknowledges the contributions of Messrs. Leonard H. Milacek and Norman Alexandre for their aid and advice on equipment problems.

The author also expresses his sincere appreciation to his wife Kun-Ai for the preparation of all figures and to Mrs. Barbara Milacek for reading the manuscript and offering corrections.

The author also wishes to acknowledge the financial support of the National Science Foundation under grant G-11769 and the School of Chemical Engineering and Materials Science Research Fund.

TABLE OF CONTENTS

		Page
LIST OF TABLES		v
LIST OF ILLUSTRATIONS		vi
Chapter		
I.	INTRODUCTION	1
II.	EXPERIMENT	19
III.	RESULTS	39
IV.	CONCLUSIONS	76
BIBLIOGRAPHY		79
APPENDICES		A-1

LIST OF TABLES

Table		Page
I.	Standard Heats of Vaporization of Mercury	8
II.	Standard Heats of Vaporization of Lead at 298°K	10
III.	Recorder Calibration	35
IV.	Torsion Constant Determination	37
V.	Cell Parameter Measurement	37
VI.	Vapor Pressure Constants of Bismuth in the Silver-Bismuth System	49
VII.	Thermodynamic Activities of Bismuth in the Silver-Bismuth Alloy	54
VIII.	Thermodynamic Activities of Silver and Bismuth at 950°K.	58
IX.	Thermodynamic Activities of Silver and Bismuth at 1000°K	59
X.	Partial Molar Entropies of Bismuth	61
XI.	The Partial Entropies of Silver at 950°K	62
XII.	Thermodynamic Properties of Silver-Bismuth System at 950°K	63
XIII.	Enthalpy and Entropy of Vaporization of Lead	66
XIV.	Heat of Vaporization of Bismuth	69
XV.	Comparison of Thermodynamic Activities at 950°K and at 1000°K	70
XVI.	Comparison of Thermodynamic Properties at 1000°K	74

LIST OF ILLUSTRATIONS

Figure		Page
1.	Diagram of Apparatus	20
2.	Operating Principle of Microbalance	25
3.	Microbalance Control System	26
4.	Circuit Diagram	30
5.	Vapor Pressure of Lead vs Reciprocal Temperature	40a
6.	Heat of Vaporization of Lead as a Function of Experimental Temperature (Third Law Calculation Method)	42
7.	Vapor Pressure of Bismuth	43
8.	Equilibrium Constants of Bismuth Vapors	45
9.	Standard Heats of Vaporization of Monatomic and Diatomic Bismuth	48
10.	Total Pressure of Bismuth in Equilibrium with Silver-Bismuth Alloys	51
11.	Monatomic Pressure of Bismuth in Equilibrium with Silver-Bismuth Alloys	52
12.	Diatomic Pressure of Bismuth in Equilibrium with Silver-Bismuth Alloys	53
13.	Activities of Bismuth and Silver in the Ag-Bi Liquid Alloys at 950°K	57
14.	Vapor Pressure of Lead vs Reciprocal Temperature	64
15.	Vapor Pressure of Bismuth vs Reciprocal Temperature	68
16.	The Comparison of Molal Enthalpies	73

A STUDY OF VAPORS OF PURE LIQUID BISMUTH AND LEAD.... SOME THERMODYNAMIC PROPERTIES OF SILVER-BISMUTH LIQUID ALLOYS

CHAPTER I

INTRODUCTION

Measurement of Vapor Pressure

Useful thermodynamic properties of a solid or liquid alloy system can be determined by equilibrating the condensed phase with the vapor phase and by measuring the equilibrium vapor pressure of the desired constituent.

Various techniques have been applied for the measurement of vapor pressure. The techniques employed can be classified into three categories: techniques in the first category are employed for the high vapor pressure range, i. e., 10^{3} mm Hg to 10^{-2} mm Hg; the second category includes techniques for the lower vapor pressure range, i. e., 10^{-3} mm Hg to 10^{-6} mm Hg; the third category includes various techniques which have been developed in order to circumvent several limitations encountered in techniques of both the first and the second category.

Some higher vapor pressure measuring methods are: (a) boiling point measurement, (b) carrier gas technique, and (c) manometer technique. These techniques usually have to be applied at comparatively high temperatures in the case of metals, because the accuracies of these techniques decrease with lower vapor pressures. Thus the low pressure methods are the most frequently used to investigate the relatively low vapor pressures of metals.

The lower vapor pressure measuring methods are based upon measurements of the rate of sublimation and vaporization. The Knudsen technique and the Langmuir technique are included in this category.

A comprehensive review of the techniques available for the measurement of metallic vapor pressure was given by Margrave (1) and Freeman (2).

In the application of the Knudsen technique, the rate of effusion can be determined either by weighing the loss of mass directly, or by weighing the condensate collected on a target adjusted to a desirable location during a known time interval. This technique is valid as long as the following fundamental requirements are fulfilled:

(a) The establishment of molecular flow of effusing vapor from the cell.

(b) The saturation of vapor with its condensed phase inside the effusion cell.

(c) The establishment of thermal equilibrium of the effusion cell.

(d) The knowledge of molecular weight of effusing vapor.

The Knudsen technique can be utilized to determine the vapor pressure of metallic vapors with reasonable accuracy.

Unlike the Knudsen technique, the equilibrium of the vapor phase with the condensed phase cannot be established in the Langmuir technique. Therefore, the rate of evaporation determined by the Langmuir technique is not always the equilibrium rate of evaporation. In other words, the evaporation pressure determined by the Langmuir technique is not always equivalent to the equilibrium vapor pressure. The deviation from maximum (or equilibrium) evaporating pressure can be taken into account by introduction of the coefficient which is called the vaporization coefficient (or condensation coefficient). Unless the vaporization coefficient is insured to be unity, the vapor pressure determined by the Langmuir technique is identically equal to $K \cdot P$ equilibrium where K, the vaporization coefficient, is less than unity and has to be determined experimentally. In order to establish the accurate measurement of vapor pressure by the application of the Langmuir technique, the following requirements must be fulfilled:

(a) The accurate measurement of the temperature of evaporating surface.

(b) The accurate determination of surface area of evaporation.

(c) The knowledge of molecular weight of evaporating vapor.

In order to circumvent the fourth fundamental requirement of

the Knudsen technique, Volmer (3) modified the original Knudsen technique so that the momentum of effusing vapor as well as the loss of material through small orifices could be determined. From the kinetic theory of gases, the pressure of vapor is related to the force exerted by the effusing vapor as:

$$dF = \frac{P \times dS}{2} \qquad (1)$$

where P is the pressure of vapor and dS is the orifice area upon which the force is exerted. To determine the force exerted by the vapor effusing through the orifices, the effusion cell is suspended by a fine wire so that the torque exerted results in the rotation of the effusion cell. If the force applied to the torsion wire is less than that required for plastic deformation, the torsional force is linearly proportional to the angle of rotation observed, and Equation 1 can be written in the following form:

$$P = \frac{2\alpha\beta}{(a_1 q_1 f_1 + a_2 q_2 f_2)} \qquad (2)$$

where a_1 and a_2 are the cross-sectional areas of the orifice holes, q_1 and q_2 are the perpendicular distances from the center of the orifice holes to the axis of rotation of the cell, α is the angle through which the cell rotates, β is the experimentally determined torsion constant of the fiber, and f_1 and f_2 are the correction factors for the effect of channel of holes (4).

In order to relate the pressure to the loss of material through

the small orifices, the Knudsen equation is derived from the kinetic theory of gases:

$$P = \left(\frac{2\pi RT}{M}\right)^{1/2} \frac{G}{(a_1K_1 + a_2K_2)} \qquad (3)$$

where R is the gas constant, T is the absolute temperature, G is the mass of effusing vapor per unit time, a_1 and a_2 are the cross-sectional areas of orifice holes, and K_1 and K_2 are the transmission coefficients (5). The transmission coefficient is the ratio of the number of molecules effusing from this cell compared to a cell of infinitesimal depth and the same area. However, the correction factor in Equation 2 is the ratio of the force resulting from the effusion through an orifice of infinitesimal depth and same area. Both correction factors fundamentally differ by the fact that the force resulting from the effusion depends on the angular distribution of effusing molecules as well as on their numbers.

These two equations are simultaneously solved to obtain the average molecular weight of effusing vapor. This molecular weight is related to the partial pressures of species in a monomer-dimer equilibrium by the following equation:

$$P_1 + (2)^{1/2} P_2 = (M/M_1)^{1/2} \cdot P \qquad (4)$$

where P_1 is the partial pressure of monomer, P_2 is the partial pressure of dimer, M is the molecular weight of the effusing vapor, and M_1 is the atomic weight of monomer.

Equation 4 thus yields the partial pressure of both species.

Since pressure equilibrium is established in the cell, the molecular weight of the vapor inside of cell is determined from Equation 5:

$$M_i = (P_1M_1 + P_2M_2)/P \tag{5}$$

where M_1 is the atomic weight of the monomer, and M_2 is the molecular weight of the dimer. If no more than two species are present in significant amounts in the pure metallic vapor, the vapor pressure of each species can be determined. The technique can be described as the torsion-Knudsen effusion-recoil method. Detailed experimental information is available from the recent work of Pratt and Aldred (6), Rosenblatt and Birchnall (7), Myles (8), Munier and Searcy (9), and in a later chapter in this thesis. Also, extensive reference is made by Freeman (2) to previous instruments and results obtained.

With equilibrium established between the monomer and dimer species over a pure metal, the pressure of monatomic vapor can be related to the pressure of diatomic vapor by the equation:

$$K_p = \frac{(P_1^{\circ})^2}{(P_2^{\circ})} \tag{6}$$

where K_p is the equilibrium constant, and P_1° and P_2° are the partial pressures of monomer and dimer in equilibrium with the pure metal phase. Likewise, for the alloy the equilibrium constant can be written as:

$$K_p = \frac{(P_1)^2}{(P_2)} \tag{7}$$

where P_1 and P_2 are partial pressures of the monomer and dimer in equilibrium with an alloy.

Assuming that the vapor behaves as an ideal gas, the thermodynamic activity of a constituent "i" in a solid or liquid solution is:

$$a_i = (P_1/P_1^o) = (P_2/P_2^o)^{1/2} \qquad (8)$$

The torsion-Knudsen effusion-recoil technique was employed in this study to determine vapor pressure and vapor atomicity of bismuth and lead in the temperature range 850°K to 1000°K. An automatic controlling-recording microbalance system was used to increase both convenience and precision. This technique was also used for measurement of thermodynamic activities in the silver-bismuth liquid alloys.

Review of the Literature

Vapor Pressure of Mercury

In the application of the torsion-Knudsen effusion-recoil technique, many measured quantities are used to determine the pressure. In order to avoid any systematic error, the apparatus must be checked against a material with a well-known vapor pressure. Also the calibration of the recorder in the microbalance system is necessary to determine what mass change corresponds to full scale deflection. Mercury was chosen for the purpose of calibration and so a brief review of the literature on mercury vapor pressure is required.

In the low temperature range, four principal investigations employing three different techniques showed excellent agreement in the standard heat of vaporization calculated by the third law method. Table I

TABLE I

STANDARD HEATS OF VAPORIZATION OF MERCURY

Source	Year	Technique	ΔH^{o}_{298} (cal/g-atom)
Neumann and Volker (10)	1932	Knudsen	14, 716 (± 53)
Mayer (12)	1931	Torsional	14, 715 (± 8)
Egerton (13)	1917	Knudsen	14, 734 (± 65)
Ernsberger and Pitman (14)	1955	Manometer	14, 660 (± 4)
Hultgren's selected value (15)			14, 691 (± 13)

shows the standard heats of vaporization by four different investigators. Values of vapor pressure determined by Ernsberger and Pitman are higher than the values determined by the three previous investigators. These earlier workers, using the Knudsen or torsional technique, improperly treated or ignored the channel effect correction factor for the orifice. Hence, there is a possibility that the vapor pressure may be higher than they reported. Furthermore, Ernsberger's and Pitman's vapor pressuresare very precise; individual pressure points do not deviate by more than 0.8 percent from the least squares equation, and also their claimed uncertainties are far less than in any other published reports.

Ernsberger and Pitman correlated their data with the following equation:

$$\text{Log P (microns)} = 11.0372 - 3,204/T \qquad (9)$$

The calculated value of vapor pressure at 30°C by Busey and Giaque (16) is approximately two percent higher than the experimental determination of Ernsberger and Pitman. An uncertainty of 1.0 to 1.2 percent would be expected in the calculated pressure, the major portion of this uncertainty being due to the lack of knowledge of the gas imperfection of mercury at the boiling point and the high pressure (14). At least, until something more is known concerning the gas imperfection of mercury at the high pressure, the values of vapor pressure determined by Ernsberger and Pitman are preferred and were utilized for this study.

Vapor Pressure of Lead

Since the vapor pressure of lead in the temperature range of concern in this study is very similar to that of bismuth, lead was selected to check the high temperature performance of the calibrated apparatus. In the range of rather high temperature, 1200°K to 1600°K, very extensive studies on the vapor pressure of lead have been performed. Except for very old investigations, the reported data on the third law values of ΔH^{o}_{298} are summarized in Table II.

Two vapor pressure investigations were found in the literature for the temperature range from 800°K to 1050°K. Egerton (13) determined

TABLE II

STANDARD HEATS OF VAPORIZATION OF LEAD AT 298°K

Source	Year	Temperature Range °K	ΔH^{o}_{298}(kcal/g-atom)
Egerton (13)	1923	800-1050	47.17 (± 0.2)
Rodebush and Dixon	1925	1400-1600	46.81 (± 0.05)
	1928	1400-1500	46.73 (± 0.05)
Harteck (19)	1928	1350-1500	46.48 (± 0.25)
Bauer and Brunner (20)	1934	1300-1600	46.37 (± 0.3)
Granovskaya and Lubmiov (21)	1953	1200-1490	46.82 (± 0.8)
Ingold (22)	1922	1200-1610	45.59 (± 0.65)
Aldred and Pratt (23)	1960	800-1050	46.81 (± 0.2)
Hultgren's selected value (15)			46.60 (± 0.3)
Stull and Sinke's selected value (24)			46.80

the vapor pressure employing the Knudsen technique. Egerton did not make a correction for a finite orifice length, and therefore, his reported vapor pressure curve is uniformly low. Egerton's early works may be recalculated to bring the vapor pressure curve to higher values by introducing the transmission coefficient for the channel effect of the orifice. Egerton also found that prolonged effusion resulted in a lowering of the pressure; hence, he could not rule out the possibility that a source of error may exist

due to undersaturation in the effusion cell. According to his report, the ratio of evaporating surface to effusion hole area is estimated to be less than ten and assuming that some minute oxide covered a portion of the evaporating surface, the ratio could be even smaller. Egerton's experiment showed that different quantities of lead in the cell produced the inconsistent values of pressure, revealing the possibility of undersaturation in the cell.

As a part of an extensive study on the thermodynamic properties of alloys, Aldred and Pratt, 1961, (23) determined the vapor pressure of lead by employing the torsional effusion technique. Their reported data of vapor pressure show some agreement with those values determined by Egerton at a lower temperature range, approximately 880°K to 920°K. However, disagreements can be observed beyond those temperatures. Aldred and Pratt's vapor pressure data are not available in the literature. If the standard heats of vaporization are calculated by means of the third law method by using chosen points of the represented equation, one can see a definite trend with temperature. For this trend which is observable in the temperature range 880°K to 1050°K,

$$\Delta H^{o}_{298} = 47.25 \text{ kcal/g-atom} \quad \text{at } 5.37 \times 10^{-7} \text{ atm } (880^{o}K)$$
$$= 46.42 \text{ kcal/g-atom} \quad \text{at } 5.22 \times 10^{-5} \text{ atm } (1050^{o}K)$$

These values are calculated by the third law method on the basis of Stull and Sinke's tabulated values of the free-energy function (24). If it is

assumed that a reasonably accurate free energy function of lead is tabulated in the above temperature range, Aldred and Pratt's equation for the vapor pressure of lead seems to raise the possibility of a temperature dependent error. More discussions are provided about this matter in a later chapter.

Hultgren et al. (15) listed the value of the standard heat of vaporization of lead to be 46.60 kcal/g-atom, giving the most weight to the data of Harteck (19) and two sets of data by Rodebush and Dixon (17, 18). On the other hand, Stull and Sinke who listed the value of 46.80 kcal/g-atom have given the most weight to the data of Rodebush and Dixon.

Vapor Pressure of Bismuth

Many investigations have been made of the vapor pressure of bismuth. However, there exist tremendous discrepancies among the reported results. Apparently these discrepancies have arisen because of inadequate application of measuring techniques to a complex situation.

Early investigation of the heat of dissociation of Bi_2 was carried out by Ko (25), employing the molecular beam technique in the temperature range from 827°C to 947°C. From the spectral distribution curves, the relative abundance of atomic bismuth and diatomic bismuth molecules in the molecular beams is reported. In calculating the heat of dissociation, the equilibrium temperatures were taken as that of the slit at the effusion chamber which was about 24°C above the temperature of the crucible. For the calculation of total pressure, crucible

temperatures were taken with an assumption that pressure equilibrium was established between the effusion chamber and the crucible. If a pressure gradient exists between the region of the slit and the crucible, it is noted that the total pressure observed is not the equilibrium vapor pressure. Ko found that diatomic bismuth molecules compose the major fraction of vapor up to 900°C and his determined heat of dissociation is 38.5 ± 0.6 kcal/g-atom of Bi. (77.0 kcal/g-mole Bi_2).

The torsion-Knudsen effusion-recoil technique was applied by Yosiyama (26) to determine the vapor pressure of bismuth and its atomicity in the temperature range 640°C to 700°C. Although his results are very precise, the calibration of the apparatus was not properly treated; the term x in Equation 2 in Yosiyama's work, that he defined as the channel correction factor, was determined by calibrating against the vapor pressure of potassium chloride with the assumption that potassium chloride vapor is monatomic. Recently, it was reported that potassium chloride vapor was composed of about 11 percent of dimer molecules at 650°C (27). It is also very hard to find the proper value of a correction factor from Yosiyama's limited information on the orifice geometry. One can conclude that there must be a possibility that systematic and temperature dependent errors are involved in Yosiyama's results.

Granovskaya and Lubmiow (28) determined the vapor pressure of bismuth in the temperature range 440°C to 705°C, by utilizing the Langmuir free-evaporation technique. Even if both the surface

temperature and the surface area for evaporation were accurately determined, the knowledge of atomicity in addition to the determination of vaporization coefficient is required to evaluate the equilibrium vapor pressure. The measured total pressure by Granovskaya and Lubmiov is $\alpha_1 P_1 + \alpha_2 P_2$; where P_1 and P_2 are the equilibrium vapor pressures of monomer and dimer, α_1 and α_2 are vaporization coefficients of monomer and dimer. In the case of bismuth vapor both α_1 and α_2 are unlikely to be unity and also are considered to be temperature dependent. Martinkevich (29) reported the mass spectrometric investigation on the relative abundance of monomer ions and dimer ions in the temperature range 340°C to 900°C. A maximum of the curve of $(I^+_{Bi_2}/I^+_{Bi})$ at approximately 500°C was observed, and the proportion of the ratio was zero at 340°C. Therefore, α_2 is clearly shown to be less than unity up to 500°C, indicating that α_2 is temperature dependent. At present α_1 and α_2 associated with evaporation of bismuth liquid cannot be determined from Martinkevich's data, but a maximum of the curve of $(I^+_{Bi_2}/I^+_{Bi})$ illustrates one of the complexities introduced into the evaporation kinetics of bismuth liquid. The measured pressure by Granovskaya and Lubimiov certainly has to be reevaluated.

The Knudsen technique was employed by O'Donnell (30) to determine the vapor pressure of bismuth in the temperature range 682°K to 771°K. He used radioactive bismuth 210 in order to improve the sensitivity of the vapor pressure determination. In analyzing his data, he

assumed that the molecular weight of bismuth in the temperature range 682°K to 771°K is 418, i. e., the molecular weight of diatomic bismuth. Although diatomic bismuth is believed to be predominant at those temperatures, O'Donnell's assumption would result in high calculated vapor pressures.

Brackett and Brewer (31) have attempted to solve the discrepencies that exist in the vapor pressure of bismuth. Observing that the evaluation of the heat of vaporization or energy of dissociation from the slope method is liable to errors due to inaccurate temperatures, they evaluated the dissociation of energy of Bi_2 by the application of the third law method to be 47.1 kcal/g-mole of Bi_2 from the correlation of three different investigations (Ko, Yosiyama, and Leu (37)). It is noted that the estimated value by Brackett and Brewer is quite different from the spectroscopic data of Almy and Sparks (32), that is, 39.6 kcal/g-mole of Bi_2.

In the study of thermodynamic properties on the uranium-bismuth alloys, Cosgarea (33) determined an apparent heat of vaporization of atomic bismuth and diatomic bismuth by utilizing the optical absorption method. The technique was utilized to measure the thermodynamic activities of alloys, and both the atomic bismuth and diatomic bismuth were detected by observing the absorption energy at the atomic absorption line and the band head for the dimer respectively. The technique requires neither a knowledge of the absolute pressure of bismuth or the

distribution of atomic bismuth and diatomic bismuth. Rice (34) unraveled the "intercept contribution" to Cosgarea's atomic bismuth vapor pressure data and redetermined the heat of dissociation to be 49.8 kcal/g-mole. The optical absorption technique does not yield a true pressure without elaborate corrections but only a quantity proportional to the pressure. Hence, a high degree of accuracy is not expected in the enthalpy of vaporization by the second law method.

Denison (35) determined the vapor pressure and atomicity of bismuth by the torque-Knudsen effusion method. His results on bismuth are inconclusive.

Recently, Aldred and Pratt (36) determined the vapor pressure of bismuth in the series of studies on thermodynamic properties of alloys by utilizing the torsional effusion technique. Their curve of vapor pressure is slightly higher than that of Yosiyama but remains lower than the extrapolated curve from O'Donnell's vapor pressure curve. Aldred and Pratt also determined the heat of dissociation of diatomic bismuth to be 47.5 kcal/gram of Bi_2 by the correlation of the Knudsen measurements of the same temperatures. More detailed discussions are provided in the later chapter.

The Silver-Bismuth System

The liquidus temperatures of this system were determined by Heycock and Neville (38), Petrenco (39), and Nathans and Leider (40). Petrenco reported a eutectic at 262°C and 95.3 atomic percent bismuth

and more recently Nathans and Leider report a eutectic at 262.5°C and 95.05 atomic percent. A portion of liquidus temperatures in this system was also determined by Kleppa (41). These reported results of liquidus temperature are in fairly good agreement.

The solidus temperature of this system has not been studied as much as the liquidus temperatures. Although disagreements in the results of solidus temperature were found, it is agreed that a retrograde solid solubility is exhibited at approximately 3 atomic percent bismuth.

Kleppa (46) determined heats of formation of liquid alloys, in the composition range from 67 to 98 atomic percent bismuth, at 723°K, utilizing the calorimetric technique. Results indicate that the maximum of the heat of formation occurs at 80 atomic percent bismuth, which amounts to 340 cal/mole.

Also, Bonnier and Desre (42) calculated the activities of silver semi-empirically at 1323°K. They applied Lumsden's equation for the excess free energy (47); at the same time, they assumed that the ideal law is obeyed within the primary solid solution of silver rich alloy. In addition to this assumption, accurate data on enthalpy of this system are needed in order to estimate a parameter in Lumsden's equation which takes into account the interaction among the next-nearest neighbor atoms. Bonnier and Desre do not give the source of the enthalpy data used in their estimate of this parameter.

Gregorczyk (43, 44) determined thermodynamic properties by

the method of measuring E. M. F. in reversible cells of the type Ag(s)| LiCl-KCl | AgBi(l) or similar cells using the corresponding bromide. Positive excess entropies of formation and positive deviations from Raoult's law in activities of bismuth were found in the temperature range from 850°K to 950°K.

Aldred and Pratt (45) determined activities of bismuth at 1000°K from the measured total pressure of bismuth. The equilibrium constant of reaction $Bi_2(g) = 2Bi(g)$ was calculated from the free energy function tabulated by Hultgren (15) and using a value of $\Delta H^{o}_{298} = 47.0$ kcal/mole of Bi_2 for the dissociation of Bi_2. Since the partial entropies of bismuth were widely scattered, they obtained activities of silver by the Gibbs-Duhem integration at 1000°K and calculated the partial free energies of silver at points along the liquidus curve by the assumption that Raoultian behavior in the silver-rich solid solution being followed. The partial entropies of silver were thus calculated from a difference in two different partial free energies at 1000°K and the liquidus temperatures. Activities of bismuth indicate a positive deviation from Raoult's law in the region of bismuth rich side of liquid alloy, but a negative deviation from Raoult's law is found in the region of silver rich side.

CHAPTER II

EXPERIMENT

Experimental Apparatus

The principal experimental apparatus consists of:

(1) a vacuum chamber, a vacuum system, and a heating furnace,

(2) an effusion cell and its suspending system, and

(3) a quartz microbalance and its automatic controlling system.

A diagram of apparatus is shown in Figure 1.

Vacuum Chamber, Vacuum System, and Heating Furnace

The evacuating system consists of a fractioning oil diffusion pump (type PMC 115, Consolidated Vacuum Co.) backed up by a mechanical vacuum pump (Welch Duo-Seal No. 1402 B). The high vacuum side of the oil diffusion pump is connected through a small side arm of the vertical chamber which is 25 mm in diameter. The upper section of a pyrex tube is 6 cm in diameter and 40 cm in length. The side arm which contains the quartz microbalance is also made of pyrex. This tube is 6 cm in diameter and 15 cm long. The brass flange is waxed by means of Apiezon W wax on to the vertical pyrex tube. The upper end of the

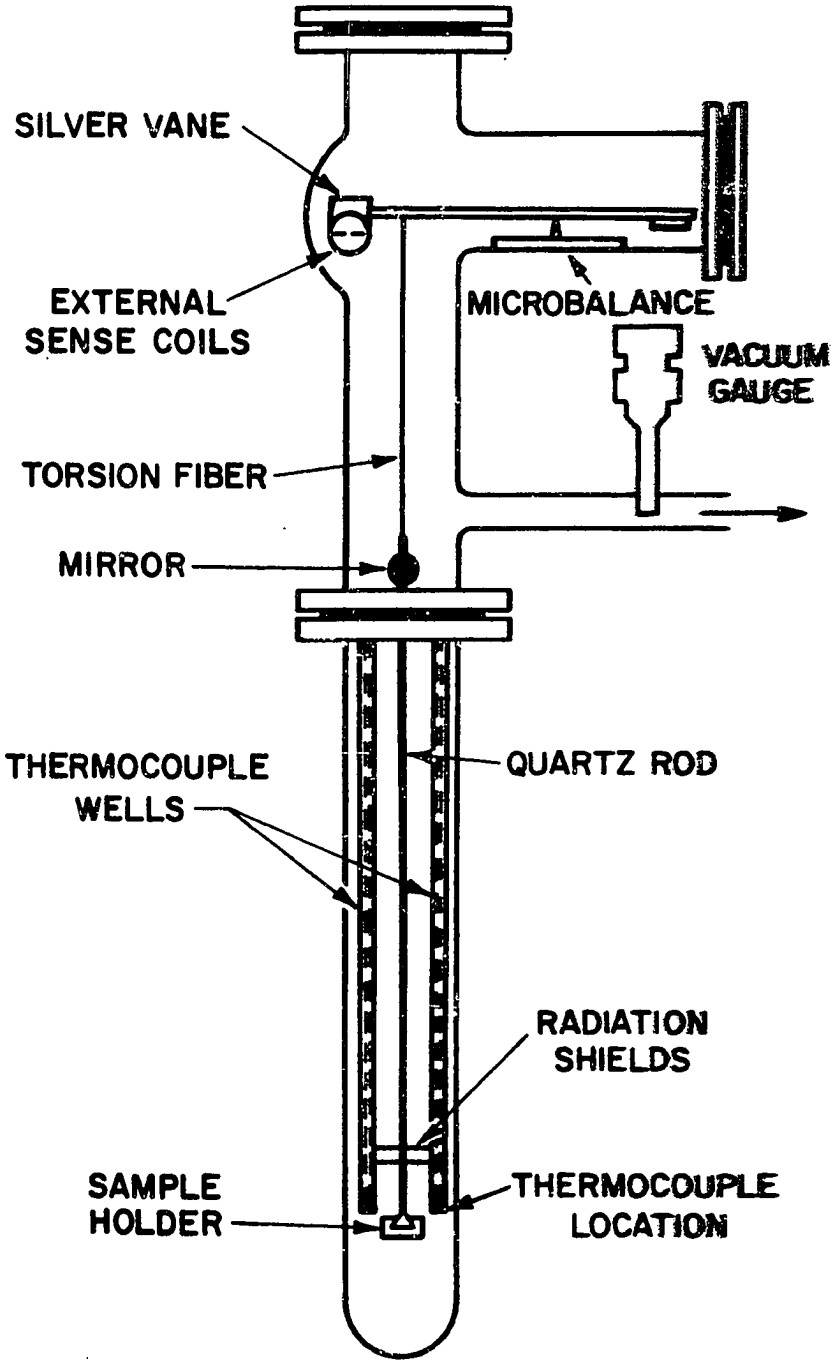

Fig. I— Diagram of Apparatus

chamber is closed by a brass plate resting freely on an O-ring. The lower section of the chamber consists of a fused quartz tube which is 5 cm in diameter and 55 cm long and is closed at the lower end. The upper end is waxed into a brass flange which is a mating flange to the end on the lower end of the upper section of the chamber. The upper and lower halves of the chamber are bolted together and the seal is provided by an O-ring. The joint between the sections of chamber is water cooled so as to keep the upper section of the chamber from becoming too hot.

Serious considerations were given to prevent vibrations or any shock from the vacuum pump or any external sources; direction propagation of vibration due to the mechanical pump to the chamber was drastically reduced by means of along rubber connections and bronze bellows. The glass system has a shock mounts to minimize vibration from the frame. The whole system is supported by the framework which is firmly fastened against the wall of the building.

The vacuum chamber is heated by a split wound resistance furnace (type MK-3010-S Hevi Duty Electric Co.) which fits around the lower section of the chamber. The furnace has three split windings--two end windings are 8 cm long and the center winding is 10 cm long giving a total heating length of 26 cm. The space between the lower chamber section and furnace windings at each end of the furnace is filled with ceramic refractory fiber so as to reduce heat loss through the ends.

The power input to the furnace is controlled by a West model

JSB-2 Proportional Controller which controls the furnace temperature to $1^{o}C$. The temperature distribution through the heated length of the furnace is further regulated by a rheostat (type 0656-10 ohm, Allied Radio Corp.) in series with each of the three furnace windings. The furnace is fitted with three Chromel-Alumel thermocouples; one near the top, one in the center, and one near the bottom. By adjusting the rheostats the maximum variance between the temperature of the three thermcouples can be reduced to $3^{o}C$ which gives a large zone in the center of the heated length where the maximum temperature variation is $\pm 1^{o}C$.

The vacuum chamber can be evacuated to $5x10^{-6}$ mm Hg in 24 hrs. The vacuum gauge used with the system is a Phillips cold cathode type, that was calibrated with a McLeod gauge in the range of pressure 10^{-4} to 10^{-6} mm Hg.

Effusion Cell and Suspending System

The effusion cell with two eccentrically located holes is suspended from a quartz microbalance by a fine torsion fiber and a rigid rod.

The effusion cells used in this experiment were made of graphite stock (Graph-I-Tite G., Graphite Specialities Corp.). The outer dimension of the cells were about 1.7 cm in length along the orifice face and 1.2 cm in width and height. A sample well was drilled lengthwise into the cell and closed by a small plug machined from the graphite stock. A typical cell weighs 4-4.5 grams.

The tungsten torsion fiber used is approximately 0.002 cm in

diameter and 20 cm in length. An aluminium disc (1 cm diameter, 0.05 cm thickness) was attached at the upper and lower part of the torsion fiber to aid in the alignment of the tungsten wire to the quartz hook, which is held with epoxy resin to the microbalance and the quartz rod below. The rod which is approximately 0.1 cm in diameter and 55 cm long is connected to the effusion cell by a triangle key block. A small galvanometer mirror (focal length 0.5 m) was attached to the rod to measure the angle of deflection of the cell using a fixed telescope and scale (Leeds and Northrup Co.). Each scale division is 0.001 radian. In addition to the thermocouples in the furnace a Chromel-Alumel thermocouple is located inside the lower vacuum chamber section with the hot junction about 0.5 cm from the effusion cell.

The Quartz Microbalance and Automatic Control System

The quartz microbalance is constructed of 2 mm diameter fused quartz rod. The balance arm is attached to the vertical supports on either side of the balance by fusing the quartz. The supporting fibers are carefully thinned until the balance has the required sensitivity.

The quartz fiber balance is continuously positioned by means of a magnetic force from a control coil on a bar magnet attached to the balance arm. Position of the balance arm is determined by a sense coil. The sense coil is a high frequency, air gap, transformer. A silver vane attached to the balance arm at the opposite end from the magnet moves in the air gap and changes the coupling between primary and secondary

of the sense coil. The signal from the secondary coil is amplified and used to generate an error signal to a servo system which controls the current to the control coil. Thus, any movement in the vane generates an error signal which causes the vane to be repositioned to zero error. The servo-system which adjusts the current required to maintain proper vane position also operates a pen recorder to record balance current in the control coil. A continuous record of control coil current is thus obtained from which rate of change of mass in the balance pan can be determined after suitable calibration. The principle of operation is shown in Figure 2.

A simplified schematic of the control system is shown in Figure 3. The controller action is such that the balance position remains constant as the load on the balance changes. A 30 KC oscillator, which is a simple free-running multi-vibrator, energizes the primary of the sense transformer. (The frequency of the oscillator is not critical since neither the primary nor the secondary of the sense transformer is tuned.) The voltage induced in the secondary of the sense transformer is dependent upon the position of the twenty mil silver vane which is attached to the balance arm and is free to move in the three-eights inch gap between the primary and secondary windings. As the vane is removed from the gap due to mass loss, less energy is dissipated by the eddy currents induced in the silver vane and more energy is transferred to the secondary of the sense transformer. The secondary output voltage is amplified

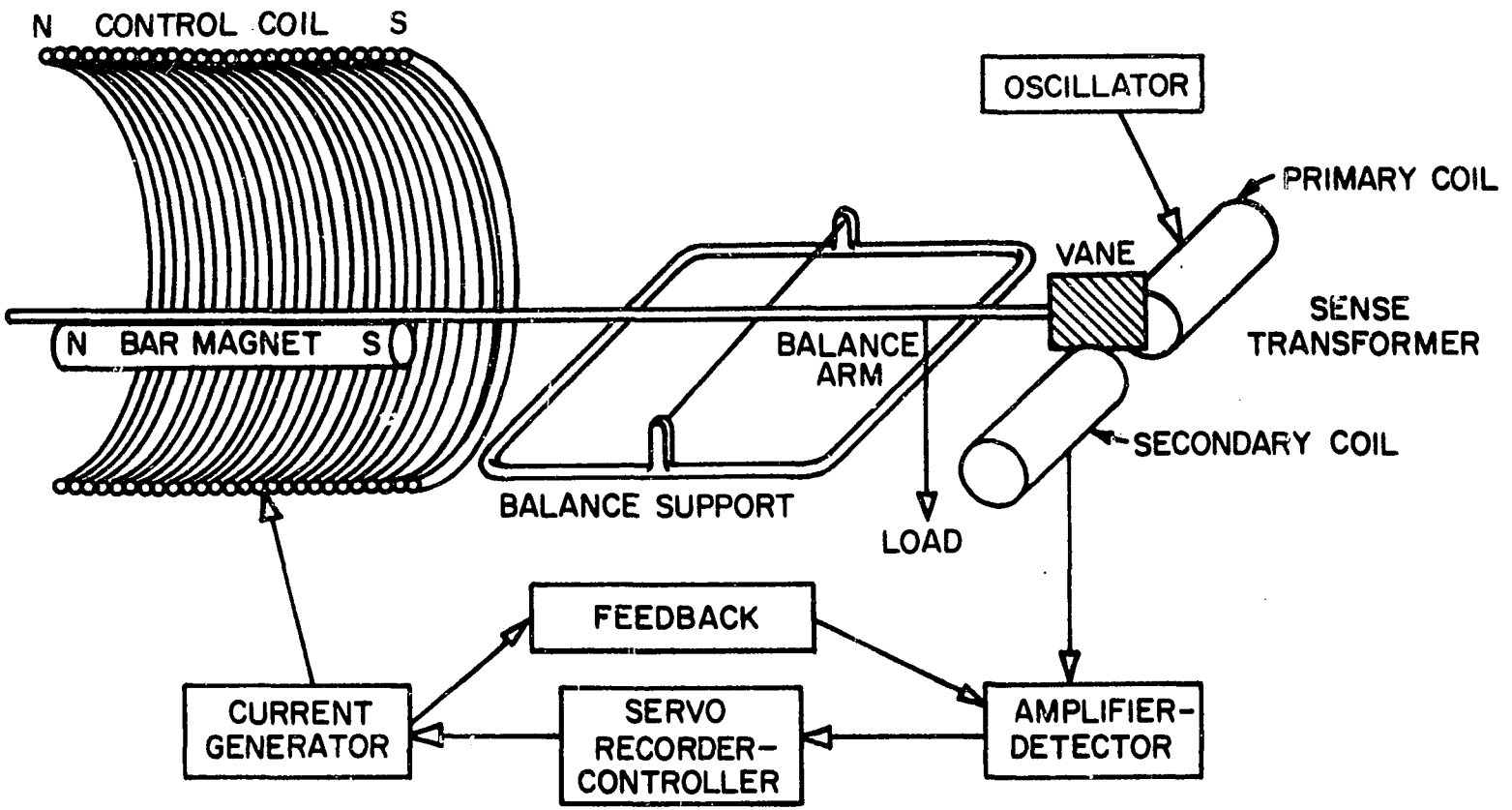

Fig. 2—Operating Principle of Microbalance

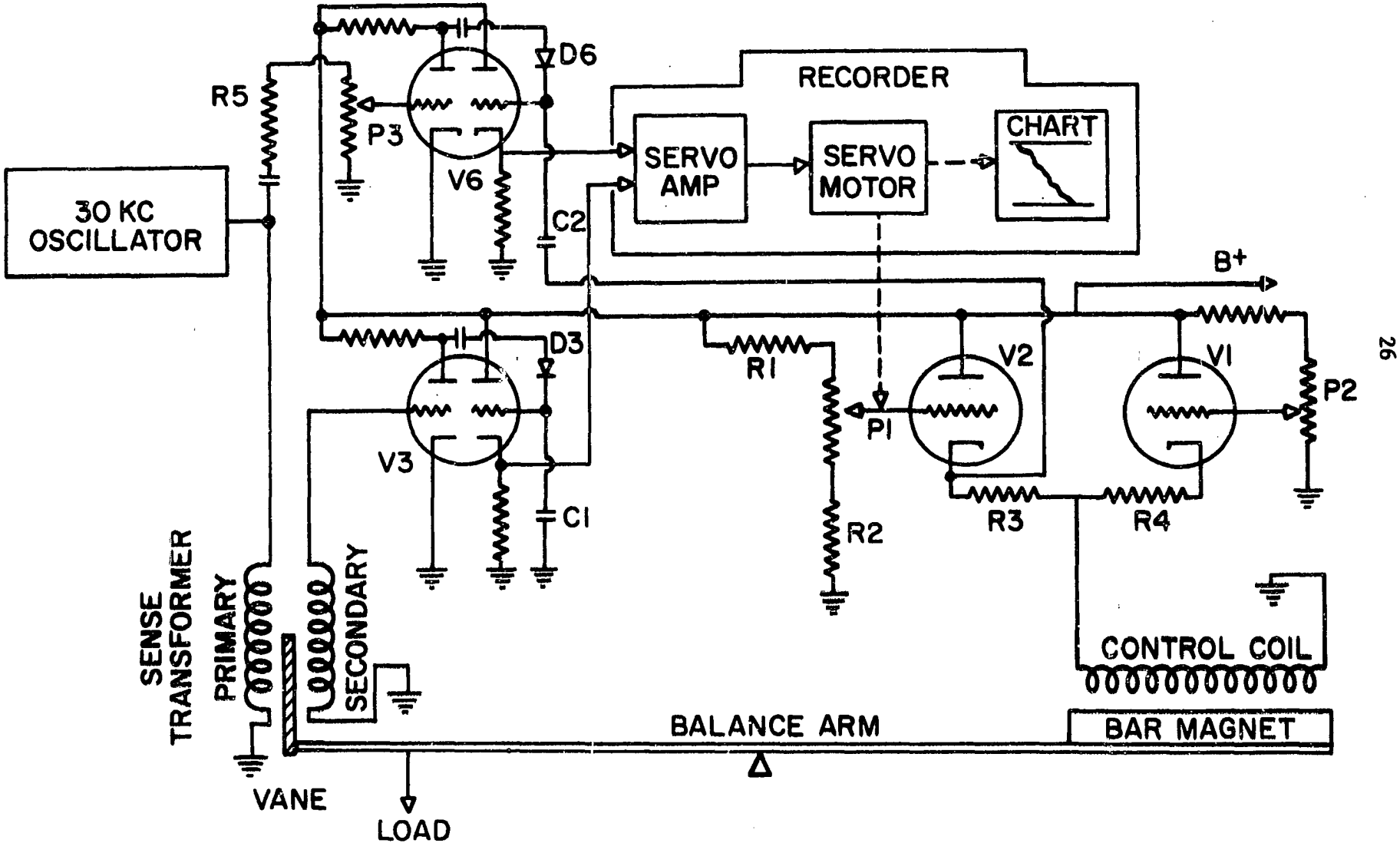

Fig. 3— Microbalance Control System

by the first half V-3, rectified by diode D-3 and fed to the input of the servo amplifier through the second half of V-3 acting as a cathode follower to match the servo amplifier input impedance. A reference voltage for the servo amplifier is developed in V-6 in the same manner that the signal voltage is developed in V-3. The reference voltage is based on the oscillator output and is amplified and rectified in the same manner as the secondary signal. By this method of developing a reference voltage, changes in amplitude of the oscillator output or change in gain of the amplifiers due to changes in plate voltage are cancelled. A potentiometer, P 3 is provided to adjust the reference to the same value as the signal voltage when the vane is the proper position between the sense transformer windings. Any difference between signal and reference voltage is amplified to provide a drive signal for the recorder servo motor. This motor changes the pen position and the setting of the balance control potentiometer, P 1. A change in the setting of P 1 changes the current through the control tube V-2 and consequently through the control coil.

The equilibrium position of the bar magnet mounted as a counterweight on the balance arm is about 1 cm below the coil axis. Any increase in current in the control coil tends to force the magnet toward the center of the coil. The magnetic force is directly proportional to the coil current for a given magnet position. The resulting balance motion moves the vane which returns the signal voltage to the same value

as the reference voltage. By means of this circuit, a null detector system is established which will maintain the vane at a constant position as the mass of the load changes.

To adjust the balance initially, a second control tube, V-1 is provided with a manually adjusted grid voltage from potentiometer P 2. P 2 is a ten turn potentiometer which allows the control coil current to be adjusted over a wide range with considerable precision. This manual control is necessary so that the various loads may be used without extremely accurate determination of initial load. It also allows the mass changes in a sample to be followed through several full automatic ranges without further mass adjustment. The magnitude of the current change in V-2, and consequently the amount of mass adjustment for the balance, is limited by the current capabilities of V-2.

The sensitivity of the system is determined by the force change possible at the control coil by full rotation of the automatic control potentiometer P 1. This, in turn, is dependent upon the voltage drop across P 1 which may be adjusted over a wide range by changes in the resistors R 1 and R 2. The present design provides a three volt drop across P 1 since R 1 is 3.9 megohms, P 1 is 0.1 megohms, R 2 is 1.0 megohms, and B + is 150 volts. The voltage drop across P 2 is 60 volts so that the manual adjustment through V-1 is approximately twenty times the automatic range.

Due to the high gain of this closed loop controller the possibility

of sustained oscillations must be considered. If the natural frequency of the undamped balance is similar to the recorder frequency, a sustained oscillation is possible. To reduce the possibility, the high frequency response of the controller was attenuated by placing a feedback capacitor, C 2, between the cathode of the control tube V-2 and the reference voltage rectifier. This capacitor was chosen to limit the pen speed to about one minute for full scale travel. This feedback accomplishes the purpose of attenuating the high frequency response of the system without limiting the low frequency sensitivity.

The long time constants limit the rate of change of mass which may be measured. Rates of change corresponding to full recorder deflection in less than five minutes should be avoided since the lag introduced by the time constants may introduce nonlinearities in the recorded signal.

A more detailed schematic of the control circuit is shown in Figure 4. The connectors shown in the schematic have the following function:

J-1 Primary of sense transformer

J-2 Secondary of sense transformer

J-3 Control coil current

J-4 A. Top of balance control potentiometer, P 1

B. Arm of balance control potentiometer, P 1

C. Ground

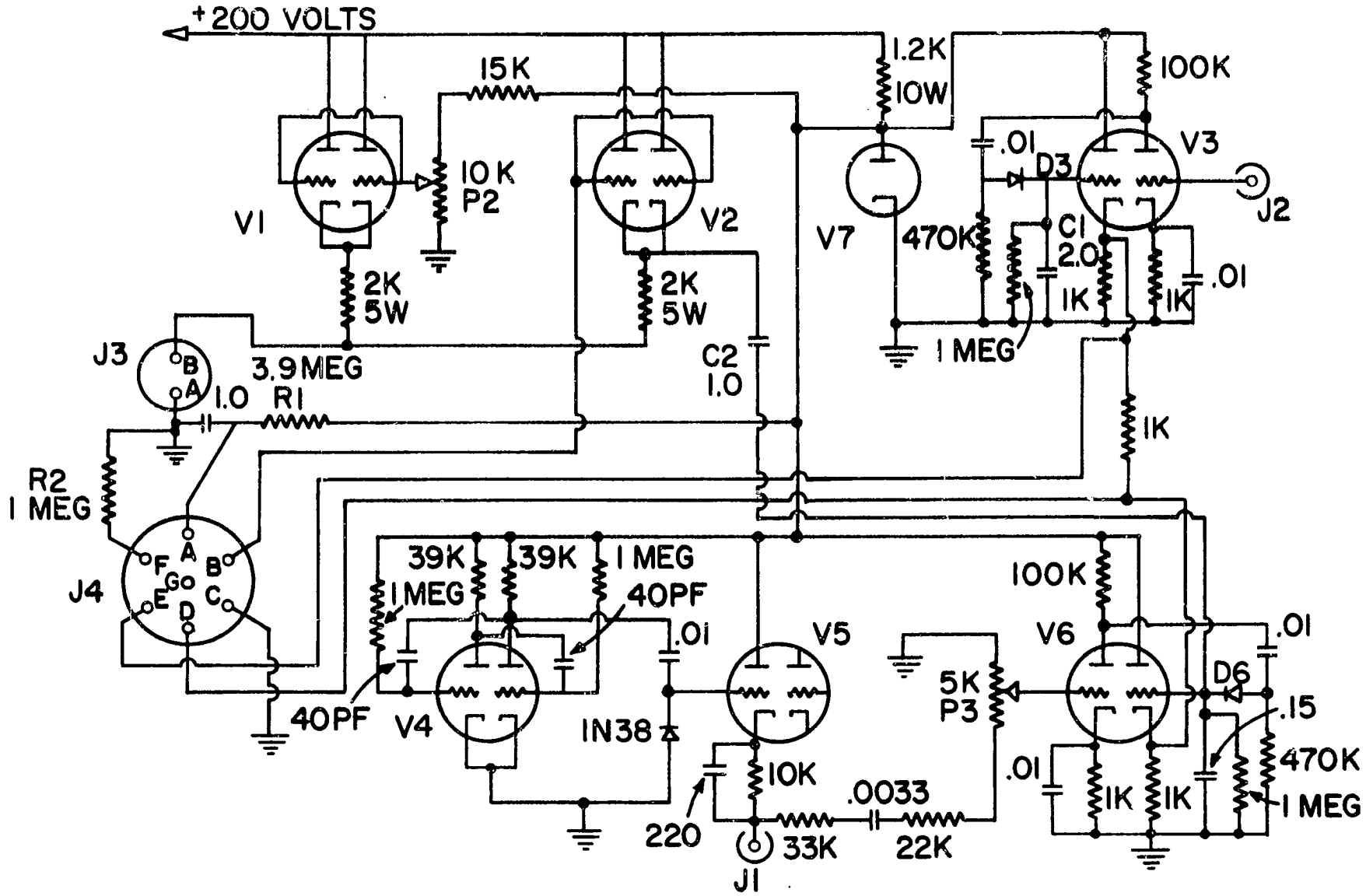

Fig. 4—Circuit Diagram

D. Reference voltage to servo amplifier

E. Signal voltage to servo amplifier

F. Bottom of balance control potentiometer, P 1

Power for the control unit is supplied from a regulated power supply. This supply furnishes the 200 volt plate voltage and 6.3 volts a.c. for the filaments. Tube V-7 is a voltage regulator tube to provide regulated 150 volts for V-3, V-4, V-5, and V-6. The tubes used are all twin triodes with the exception of V-7. V-4 is a 12Ax7 and the others are 12AU7.

Experimental Procedure and Calibration of Apparatus

Preparation of Metal Samples

The metals used in this experiment were 99.999% pure bismuth, 99.999% pure lead, and 99.999% pure silver by spectrographic analysis. The pure bismuth and the pure silver were obtained from the American Smelting and Refining Co. and the pure lead from the Consolidated Mining and Smelting Company, Limited. Mercury which was used in the calibration of the apparatus was Fisher reagent chemical grade.

Bismuth samples or lead samples were immersed in 1 to 1 diluted hydrochloric acid for about 5 to 10 minutes and washed thoroughly with distilled water. The washed sample was dried by blowing air immediately before the specimen was placed in the effusion cell.

When mercury was used in the experiment, special care was

taken to avoid contamination by dust. Since it was found that dust particles in the effusion cell easily stick upon the surface of mercury specimen, the effusion cell was cleaned with a small brush before the mercury was put in.

For preparation of alloy samples, a capsule shaped quartz tube (1 cm dia.) was filled with a weighed quantity of silver and bismuth. Precautions similar to those used with other pure metals were taken to remove any trace of oxide from the granular bismuth. The open end of the capsule was fused to a vacuum system which is capable of evacuating well below 10^{-5} mm Hg. When a desired vacuum was obtained, the capsule was fully outgassed for 30-40 minutes with a mild flame. The capsule was then fused off from the vacuum system.

The ampoule thus prepared was heated in the mufile furnace to a temperature approximately 100°C above the alloy liquidus point and held for three hours. From time to time, the ampoule was vigorously shaken to homogenize the liquid alloy. The liquid alloy in the ampoule was quenched in the water, and the rod of alloy sample was kept under vacuum until required.

Experimental Procedure

The sample was placed in the effusion cell which was then fixed to the suspension system. A quantity of the specimen was added or subtracted to adjust the recorder pen with the potentiometer of the automatic controller set at zero.

Initial heating to 200°C caused a deflection of the cell which was presumably due to absorbed gas. This initial deflection of the cell did not remain longer than 15 minutes, and the cell position gradually returned to the original reading of the zero point. The original reading of the zero point was insured to be true by checking whether the applied electrostatic or electromagnetic field surrounding the effusion cell in the furnace interacts with the effusion cell. The test consisted of turning the furnace on and off, since it was expected that the zero point of suspension system might vary to some degree with the electromagnetic field being applied by the heating element of the furnace.

The furnace was heated rapidly and automatically controlled to a desired temperature. It was allowed to heat for ten to twenty minutes to achieve thermal equilibrium of the effusion cell before any data were taken. When the suspension system indicated a constant deflection, the pen position of the recorder was readjusted to zero. The deflection of the suspension system was determined and continuously observed while the recorder sensed the mass loss of the cell. Before each experiment, the effusion cell was outgassed and heated to 850°C for 10 hours under a vacuum of 5×10^{-5} mm Hg.

A small air blower was utilized to cool the section of the lower chamber immediately above the top of the furnace. This resulted in vapor condensation on the tube walls within a short vertical distance above the top of the furnace. The condensation of vapor onto the quartz rod

was not observed at a vapor pressure lower than 10^{-2} mm Hg.

The thermocouple was made from matched Alumel-Chromel wire (3G-170 Hoskins Manufacturing Co.) which was calibrated against the melting points of zinc and silver. The thermocouple was also calibrated with standard thermometers (Brooklyn Thermometer Co.) in the temperature range of 25°C to 45°C using the water bath which controlled the temperature within 0.05°C.

Calibration of the Cell Constants and the Quartz Microbalance

The orifice area was determined by taking photographs at a calibrated magnification (75x) with a metallographic microscope. The image was projected onto calibrated graph paper for the counting of squares method. The accuracy of the area determined by this method is $\pm 10^{-5}$ cm^2.

The depth of the orifice was determined by a metallographic microscope by focusing on the surface of edge and then refocusing on a brass surface which was placed inside the cell and held tightly against the inside edge of the orifice. The accuracy determined by this method is $\pm 10^{-3}$ cm.

The recorder in the microbalance system was calibrated to determine the mass change corresponding to full scale deflection. Since it was necessary to calibrate the recorder for mass effusion rates of the same order encountered in this study, it was desirable to use data on a substance with a similar atomic weight at a temperature where its

vapor pressure concided with the vapor pressure range of interest (10^{-4} to 10^{-2} mm Hg). Mercury was chosen as the calibrating substance because it met the above stated requirements and excellent vapor pressure data in the range of 10^{-4} to 10^{-2} mm Hg was available. Also, because mercury has such a small amount of Hg_2 present in the vapor even at a temperature up to the boiling point, its molecular weight may be taken as the atomic weight (within 0.05%) (24).

For the calibration an insulated water bath which could be controlled to $\pm$ 0.05°C was utilized instead of the furnace. The mercury sample was brought to the desired temperature, and the time required to reach full scale deflection of the recorder was observed. The mass effusion rate was used to calculate the total mass loss for full scale deflection. Six calibration values were obtained from mercury vapor pressure data utilizing three effusion cells. The results are shown in Table III. The basic data on cell constants used in the calculation of weight

TABLE III

RECORDER CALIBRATION

Cell	Weight Loss (grams) Full Scale Deflection
A	2.069×10^{-3}
	2.010×10^{-3}
B	2.036×10^{-3}
	2.047×10^{-3}
C	2.051×10^{-3}
	2.068×10^{-3}
Average	2.047×10^{-3}

loss are shown in Appendix A. An estimate of the transmission coefficients were made from the simplified equation by Kennard (52).

Torsion Constant

The period formula for angular harmonic motion is,

$$t = 2\pi\left(\frac{I}{\beta}\right)^{1/2} \tag{10}$$

where β is torsion constant; t, period of oscillation; and I, moment of inertia of pendulum with a known weight. The determination of the torsion constant is achieved by measuring the period of suspension system alone and with a brass weight attached. Thus β is calculated as:

$$\beta = \frac{4\pi^2 I_w}{t_w^2 - t^2} \tag{11}$$

where I_w is the moment of inertia of the brass weight, t_w is the period of the suspension system with the brass weight and t is the period of the suspension system alone. The added brass weight was a cylinder of 2.520 grams with its diameter 0.632 cm. The data showing a typical determination of the torsion constant for a tungsten fiber (0.002 cm in diameter and 20 cm long) is given in Table IV. After all experimental runs, the determination of torsion constant was rechecked and showed no significant changes. The torsion constant thus determined was calculated to be 0.118 dyne-cm/radian.

As a check on the measurement of cell parameters performed optically, the value of $(a_1q_1f_1 + a_2q_2f_2) = 2\beta\alpha/P$ was determined from

mercury vapor pressure data with ς = 0.118 obtained. Instead of trying to obtain a "zero point" for the suspension, the sum was calculated using the vapor pressure at two different temperatures and the corresponding angles of deflection. The results are presented in Table V.

TABLE IV

TORSION CONSTANT DETERMINATION

	Suspension System Alone t (sec)	Suspension System with Brass Weight t_w (sec)
5 periods	29.54	43.75
10 periods	59.06	87.74
An average period	5.91	8.77

TABLE V

CELL PARAMETER MEASUREMENT

	$(a_1q_1f_1 + a_2q_2f_2)\ cm^3$	
Cell	Optical	Mercury Data
A	2.492×10^{-3}	2.530×10^{-3} 2.482×10^{-3}
B	4.309×10^{-3}	4.315×10^{-3} 4.195×10^{-3}
C	5.529×10^{-3}	5.466×10^{-3} 5.590×10^{-3}

The cell parameter $(a_1q_1f_1 + a_2q_2f_2)$ which is obtained from the optically measured values and the proper application of Searcy-Freeman's correction factor, is very close to the values obtained for the calibration with mercury. No systematic variation in the mercury data was observed, proving that the optically measured values in the cell parameter are valid within the error limit of the experiment. To use the cell parameter at high temperatures, these dimensions were corrected for the effect of expansion at each experimental temperature.

CHAPTER III

RESULTS

The partial pressure of the monomer and dimer were calculated from each measurement of total pressure and effusion rate. These values were used to determine the heats of vaporization by the third law method. In addition, a least square treatment of the monomer pressure, dimer pressure, and total pressure was performed on the IBM 1410. The generalized from of the equation used for the correlation of the data is:

$$\log P = - A/T + B \log T + C \qquad (12)$$

Three control conditions have been imposed in the least squares treatment, Control Condition One is an unrestricted determination of A, B, and C. The B coefficient in the above equation is equivalent to the value of $(C_{p_v} - C_{p_l})/R$, that is, the heat capacity difference between a substance in the vapor state and in the liquid state. In Control Condition Two, the B value is fixed from C_p data presented in Stull and Sinke (24). A different value of B is also used to yield new values of A and C based on the vapor species data from Stull and Sinke and condensed state data from the recent publication, Bell and Hultgren (11). B is set equal

to zero in Control Condition Three. Control Condition Three implies that the heat of vaporization is independent of temperature over the range of the experimental temperatures.

The uncertainties indicated in these sections are 95% confidence limits calculated from the deviations of arithmetic means.

Results of Lead

The results obtained for the total pressures of lead are shown in Figure 5. A least squares treatment in Control Condition Two yields:

$$\log P(\text{atm}) = (4.984 \pm 0.132) - (9,760 \pm 121)/T \qquad (13)$$

At 800°K the specific heat difference of lead from its liquid state to vapor state is taken to be -2.2 cal/deg g-atom (15). Since it is assumed that this difference remains fairly constant over the temperature range from 800°K to the experimental temperature, the correlation of data can be given as:

$$\log P(\text{atm}) = (-10,186 \pm 119)/T - 1.1071 \log T + (8.728 \pm 0.123) \qquad (14)$$

In addition, a least squares treatment in Control Condition One yields:

$$\log P(\text{atm}) = (-9,379 \pm 438)/T + (0.9538 \pm 1.072)\log T + (1.7429 \pm 3.621) \qquad (15)$$

Among three different control conditions, Equation 14 shows

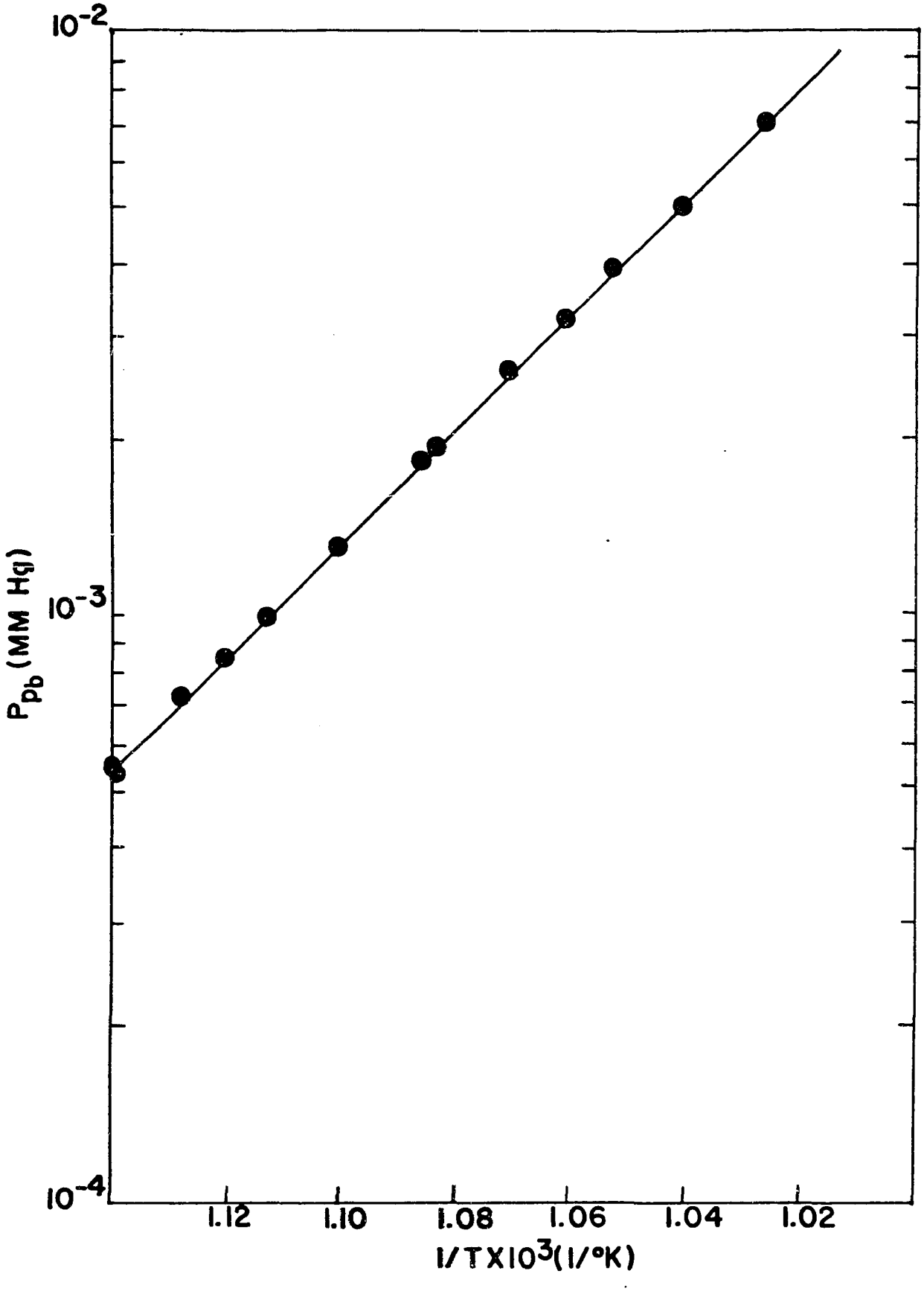

Fig. 5— Vapor Pressure of Lead vs Reciprocal Temperature

the best correlation with the data. It is noted that the B coefficient determined by Control Condition One does not have any physical significance since $B = (C_{p_v} - C_{p_e})/R$ is negative, and also it is apparent that the B coefficient determined by Control Condition One is highly insignificant at the level of 95% confidence limit.

Figure 6 shows the values of the standard heats of vaporization of lead at 298°K as a function of experimental temperature. The Third Law calculation method was used. The average value of the standard heats of vaporization is 46.60 ± 0.02 kcal/g-atom, and no discernible trend with temperatures is observed.

The average molecular weight of the effusing vapor was 207.4 ± 2.27. Hence, within the temperature and detection limits of the experiments performed, the lead vapor was found to be monatomic over the temperature range 870°K to 980°K.

The experimental data for lead from which results above are calculated are shown in Appendix B.

Results for Bismuth

The results obtained for the total pressure, monatomic pressure, and diatomic pressure are shown in Figure 7.

Least square treatments of the data in the form of the Clasius-Clapeyron equation yields the following correlations for total pressure, monatomic pressure, and diatomic pressure:

$$\log P_T(\text{atm}) = (5.24 \pm 0.24) - (9,656 \pm 218)/T \qquad (16)$$

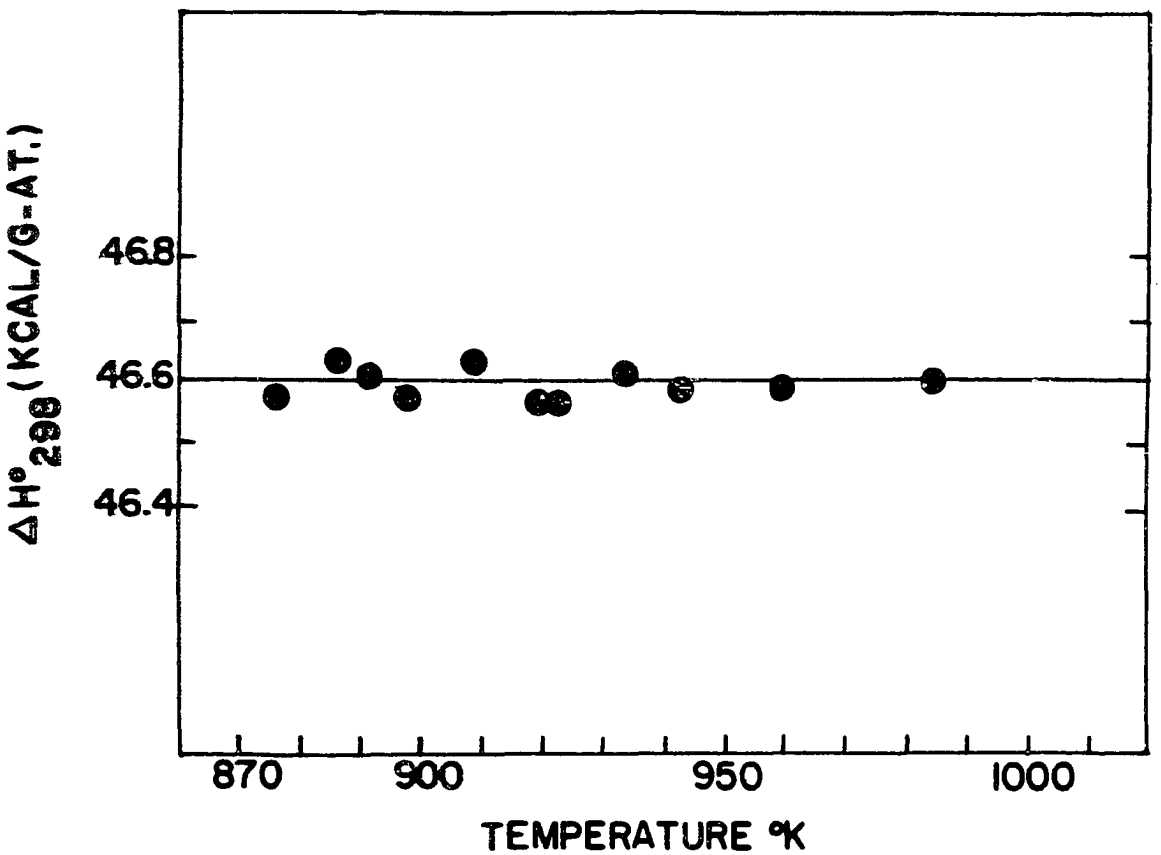

Fig. 6— Heat of Vaporization of Lead as a Function of Experimental Temperature (Third Law Calculation Method)

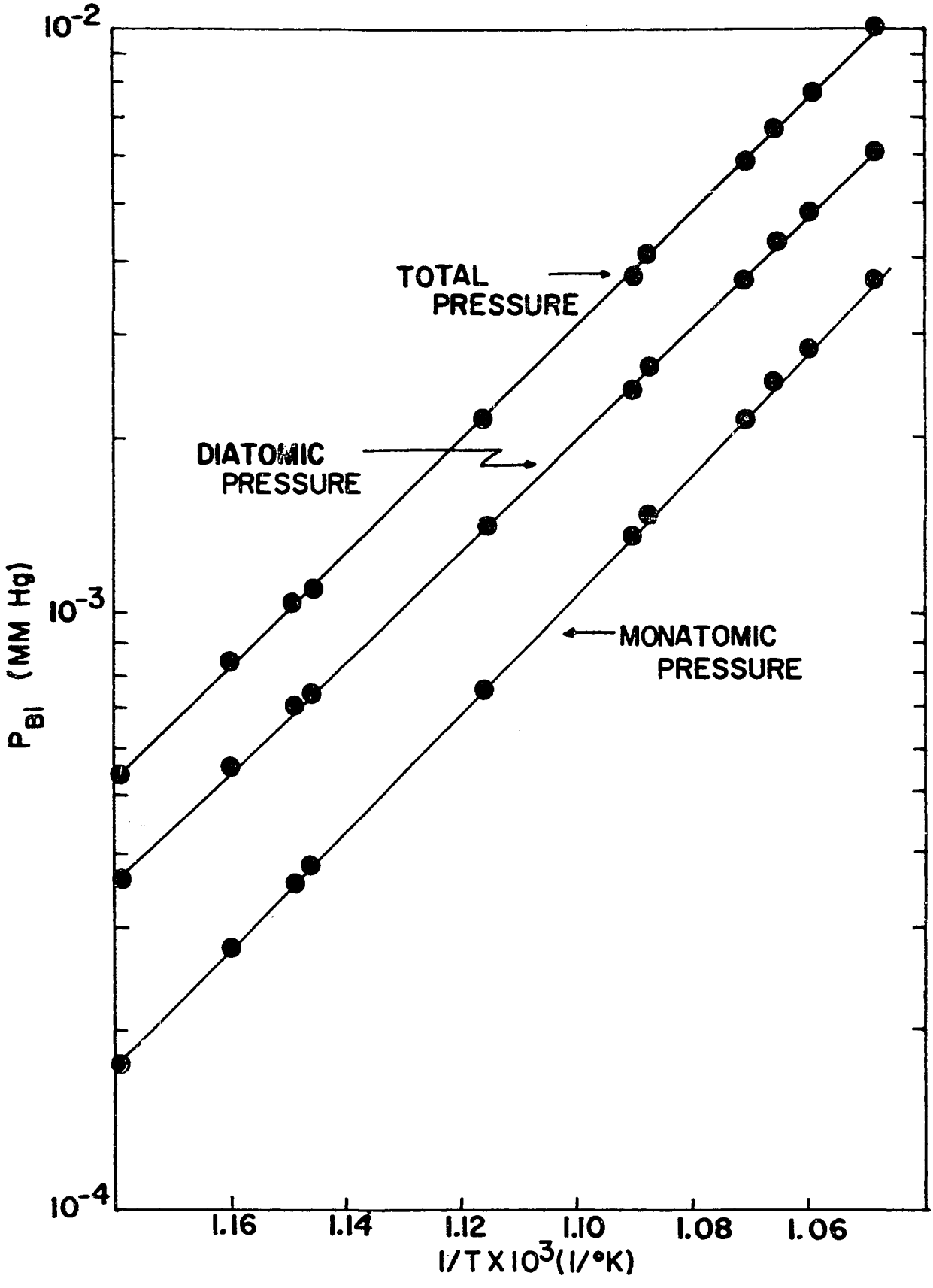

Fig. 7— Vapor Pressure of Bismuth

$$\log P_1(\text{atm}) = (5.27 \pm 0.28) - (10,100 \pm 253)/T \quad (17)$$

$$\log P_2(\text{atm}) = (4.78 \pm 0.23) - (9,418 \pm 211)/T \quad (18)$$

Assuming that the specific heat difference from bismuth liquid to its vapor state is -2.53 cal/g-atom at 600°K (24), the least square treatment yields the correlation of data monatomic bismuth vapor pressures as:

$$\log P(\text{atm}) = (-10,597 \pm 253)/T - 1.273 \log T + (9.591 \pm 0.280) \quad (19)$$

and also from the data of diatomic pressures as:

$$\log P(\text{atm}) = (-10,616 \pm 213)/T - 3.064 \log T + (15.174 \pm 0.236) \quad (20)$$

The combination of Equations 19 and 20 yields the equilibrium constant as the following relationship:

$$\log K_p(\text{atm}) = (-10,578 \pm 258)/T - 0.518 \log T + (4.008 \pm 0.286) \quad (21)$$

A plot of $\log K_p$ versus $1/T$ is shown in Figure 8.

Constants A, B, and C which are determined in the least square treatment of total vapor pressure, monatomic pressure and diatomic pressure as an unrestricted control condition yields the following relationships:

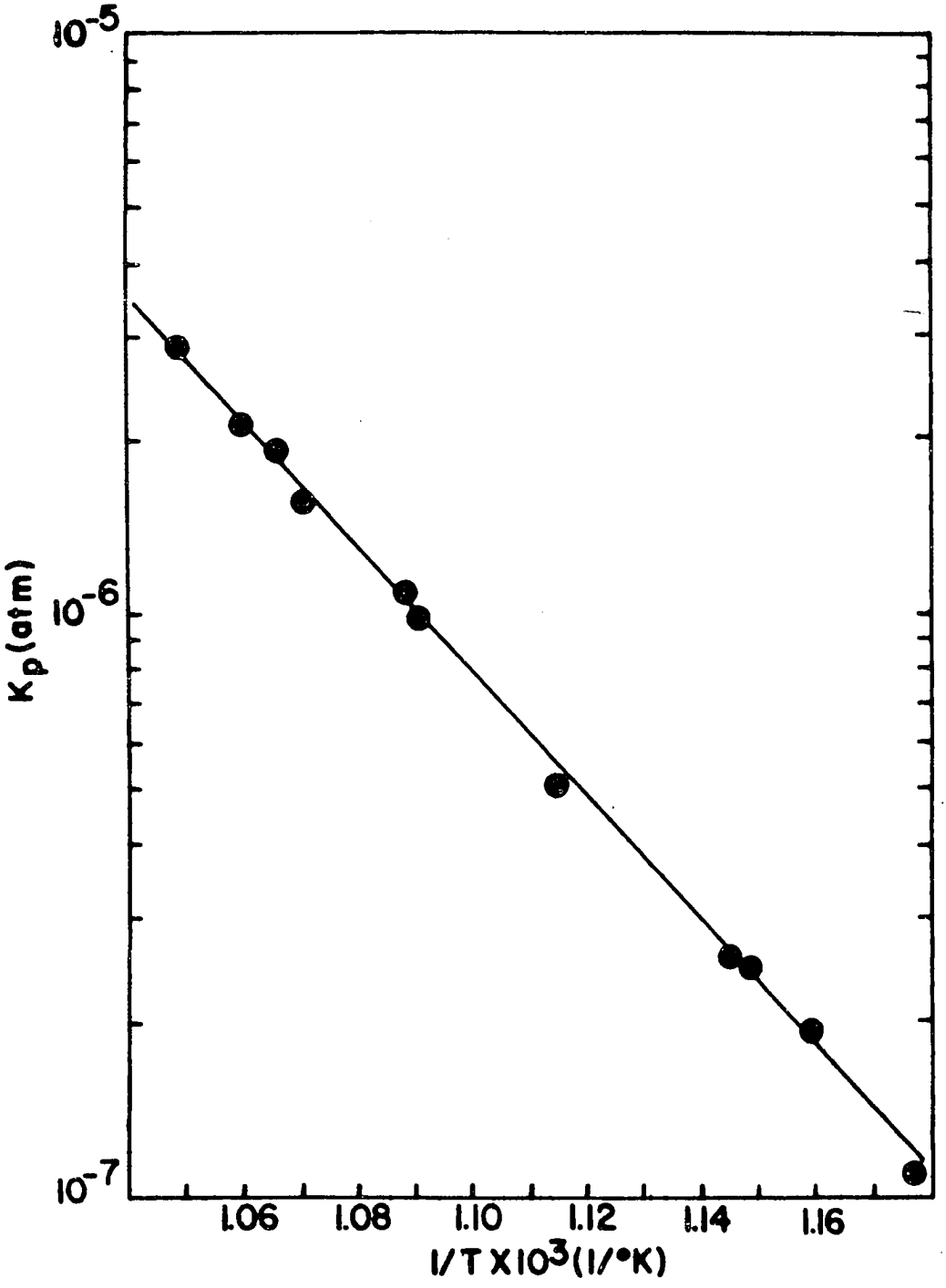

Fig. 8—Equilibrium Constants of Bismuth Vapors

$$\log P_T(\text{atm}) = (-76,538 \pm 1,516)/T + (5.12 \pm 3.83)\log T - (12.13 \pm 7.78) \quad (22)$$

$$\log P_1(\text{atm}) = (-9,839 \pm 2,232)/T + (0.66 \pm 5.64)\log T + (3.01 \pm 11.45) \quad (23)$$

$$\log P_2(\text{atm}) = (-6,912 \pm 2,925)/T + (6.41 \pm 7.39)\log T + (16.94 \pm 15.00) \quad (24)$$

Using the heat capacity data of liquid bismuth by Bell and Hultgren (11), the average specific heat of liquid from 850°K to 950°K is estimated to be 6.63 cal/g-atom. With the aid of the tabulation of gaseous species from Stull and Sinke (24), a least squares treatment of monatomic bismuth pressure and diatomic pressure yield for the control condition of fixing the B coefficient:

$$\log P_1(\text{atm}) = (-10,426 \pm 253)/T - 0.8353 \log T + (8.108 \pm 0.280) \quad (25)$$

$$\log P_2(\text{atm}) = (-10,268 \pm 212)/T - 2.1738 \log T + (12.155 \pm 0.235) \quad (26)$$

The combination of Equations 25 and 26 yields for the equilibrium constant the following relationship:

$$\log K_p(\text{atm}) = (-10,586 \pm 258)/T - 0.5032 \log T + (4.061 \pm 0.286) \quad (27)$$

Also the combination of Equations 17 and 18 yields for the equilibrium constant the following relationship:

$$\log K_p(\text{atm}) = (-10,782 \pm 396)/T + (5.766 \pm 0.439) \qquad (28)$$

Control Condition Two as well as Control Condition Three yield better fits of data than Control Condition One. Likewise in the treatment of Lead data, the B coefficient determined by Control Condition One is highly insignificant at the level of 95% confidence limit. This matter is discussed in detail in the later section.

Experimentally determined molecular weights of bismuth vapor inside the cell over the temperature range 850°K to 950°K, can be correlated by the following equation:

$$\log M = (93.611 \pm 3.546)/T + (2.4335 \pm 0.0039) \qquad (29)$$

Although the above equation fits the experimental data very well, caution should be taken in calculating molecular weights at temperatures appreciably different from the experimental temperature.

The standard heats of vaporization of both monomer and dimer are calculated and shown versus temperatures of experimental determinations in Figure 9. The average values of the standard heat of vaporization are estimated on the basis of Hultgren and Bell's data:

$$\Delta H^{\circ}_{298} \text{ (monomer)} = 50.18 \pm 0.07 \text{ kcal/g-atom}$$

$$\Delta H^{\circ}_{298} \text{ (dimer)} = 52.83 \pm 0.09 \text{ kcal/g-atom}$$

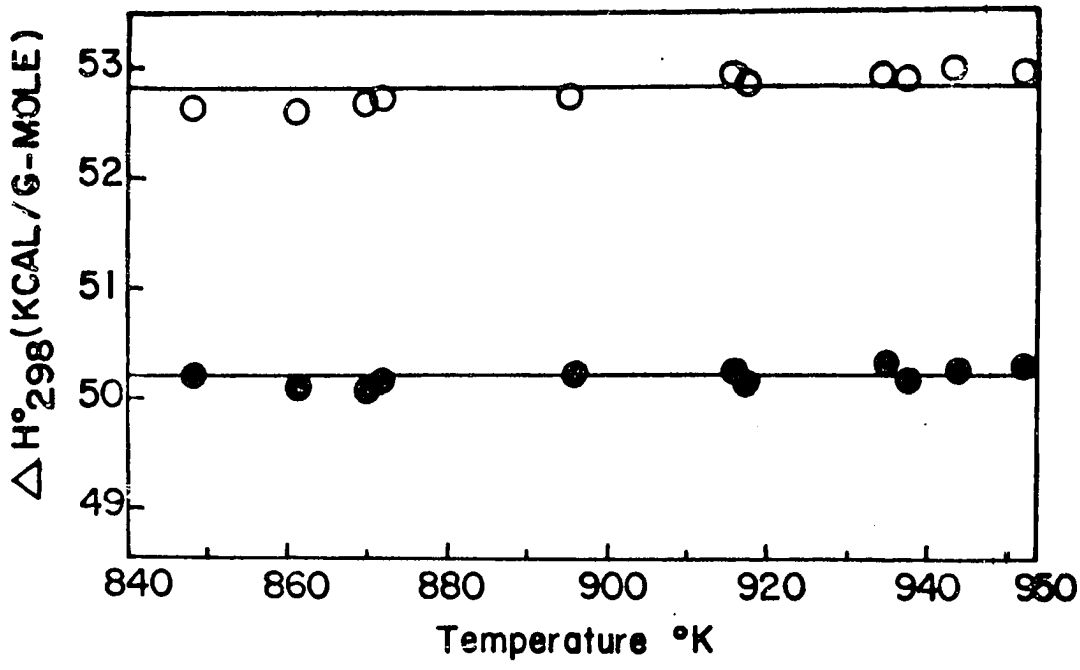

Fig. 9—Standard Heats of Vaporization of Monatomic and Diatomic Bismuth

LEGEND ○ Dimeric Vapor
● Monomeric Vapor

These results correspond with dissociation energy of diatomic bismuth as 47.53 kcal/g-mole of Bi_2 at 298°K.

The experimental data for bismuth from which results above are calculated are shown in the Appendix C.

Results for Bismuth-Silver Alloys

The vapor pressures of bismuth for various liquid alloys are shown graphically in Figure 10. Monatomic and diatomic pressures of bismuth for alloys are also shown respectively in Figure 11 and Figure 12. The data are fitted by a least square treatment to the Clasius-Clapeyron equation. Table VI shows a summary of these results for total pressure,

TABLE VI

VAPOR PRESSURE CONSTANTS OF BISMUTH IN THE SILVER-BISMUTH SYSTEM

Top Values from Monatomic Vapor Pressure
Middle Values from Diatomic Vapor Pressure
Bottom Values from Total Vapor Pressure

Alloy Composition (N_{Bi})	Range of Temperature (°K)	$A \times 10^{-4}$*	$C \times 10^{-1}$*
0.865	892-953	1.0101 ± .208	.523 ± .023
		.9356 ± .207	.463 ± .023
		.9640 ± .206	.515 ± .022
0.790	889-951	1.0133 ± .172	.524 ± .018
		.9345 ± .173	.457 ± .018
		.9652 ± .140	.512 ± .015
0.682	890-961	1.0009 ± .230	.508 ± .037
		.9227 ± .343	.439 ± .055
		.9547 ± .303	.496 ± .049

TABLE VI--(Continued)

Alloy Composition (N_{Bi})	Range of Temperature (^{o}K)	A x 10^{-4} *	C x 10^{-1} *
0.522	897-972	1.0075 ± .241	.506 ± .026
		.9167 ± .293	.416 ± .031
		.9584 ± .273	.487 ± .029
0.400	917-974	.9827 ± .523	.460 ± .051
		.8799 ± .728	.336 ± .071
		.9404 ± .579	.438 ± .056
0.311	922-990	.9827 ± .130	.460 ± .014
		.8799 ± .340	.336 ± .036
		.9404 ± .217	.438 ± .022
0.290	923-973	.9783 ± .446	.451 ± .046
		.9239 ± .402	.372 ± .042
		.9571 ± .584	.450 ± .061
0.229	946-1002	.9948 ± .330	.443 ± .034
		.9174 ± .737	.316 ± .075
		.9752 ± .415	.435 ± .042
0.080	942-1003	.7389 ± .240	.167 ± .025
		.4125 ± .226	-.226 ± .023
		.6710 ± .150	.107 ± .016

*$\log P(atm) = - A/T + C$

N_{Bi}: mole fraction of bismuth

monatomic pressure, diatomic pressure. Thermodynamic activities of bismuth were calculated by Equation 8 or by utilizing both the equilibrium constants of bismuth vapor and the measured total vapor pressure for alloys. The equilibrium constants K_p of bismuth vapor were calculated from Equation 28; the calculated values of K_p at $850^{o}K$, $900^{o}K$, $950^{o}K$,

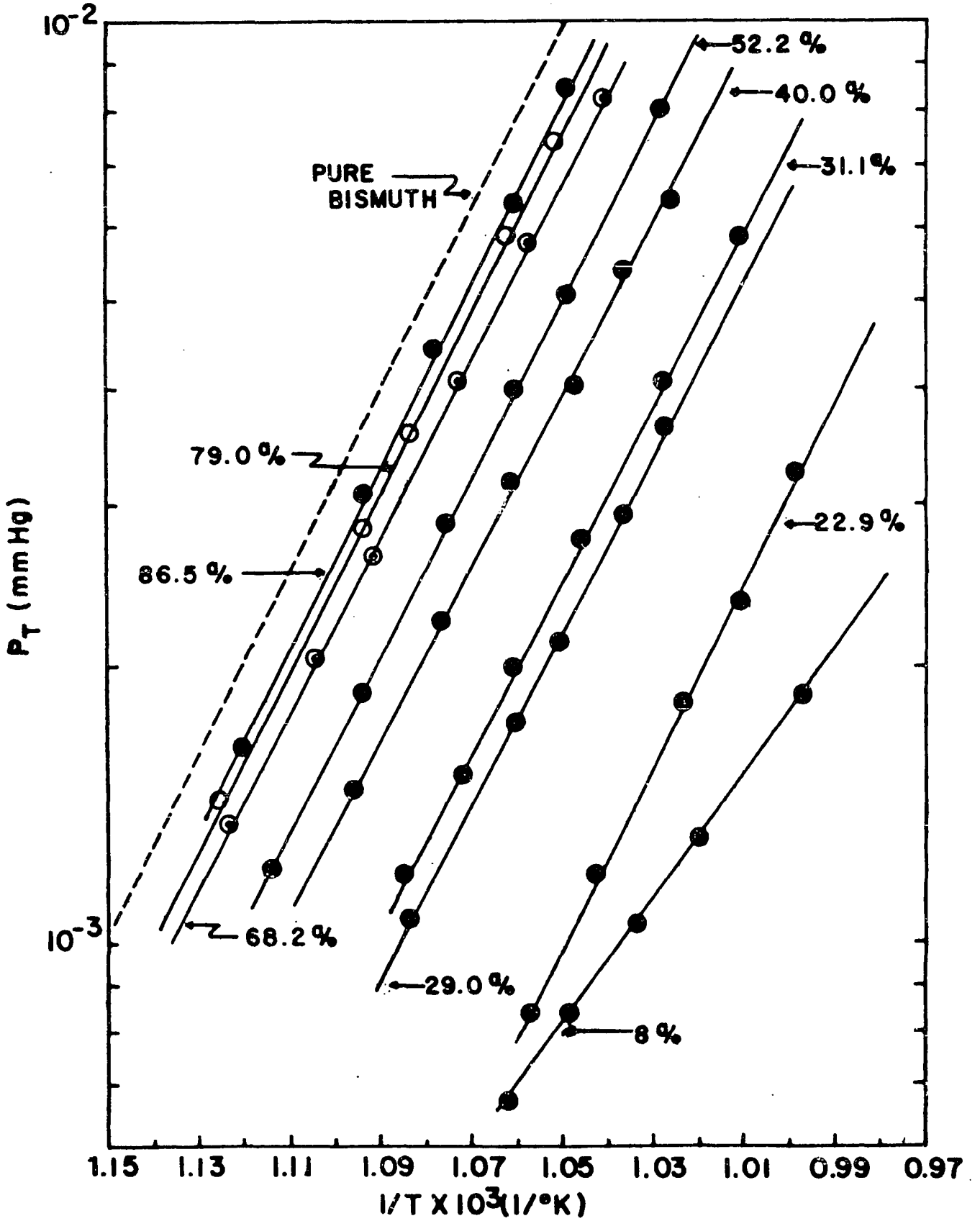

Fig. 10– Total Pressure of Bismuth in Equilibrium with Silver–Bismuth Alloys

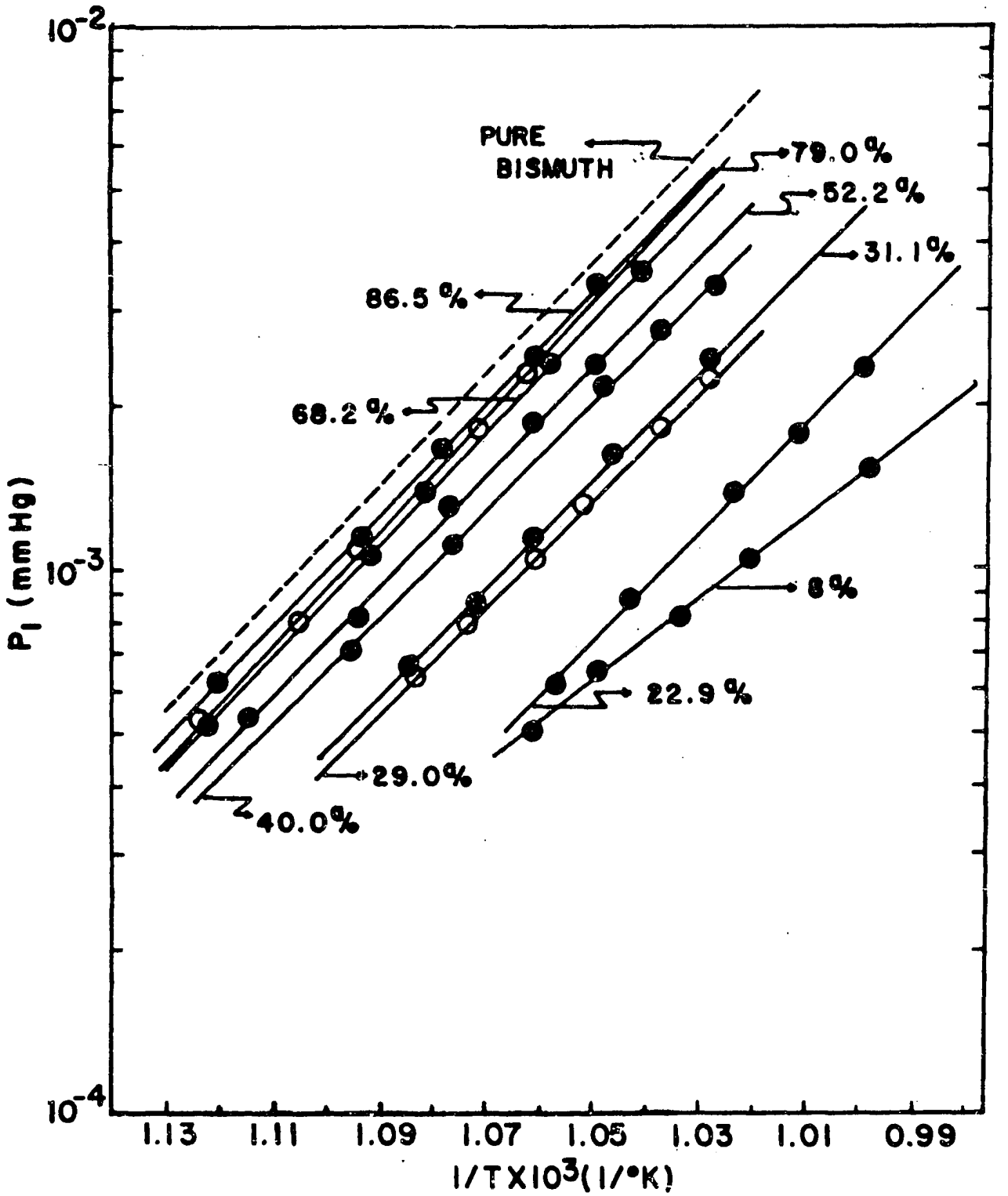

Fig 11 – Monatomic Pressure of Bismuth in Equilibrium with Silver - Bismuth Alloys

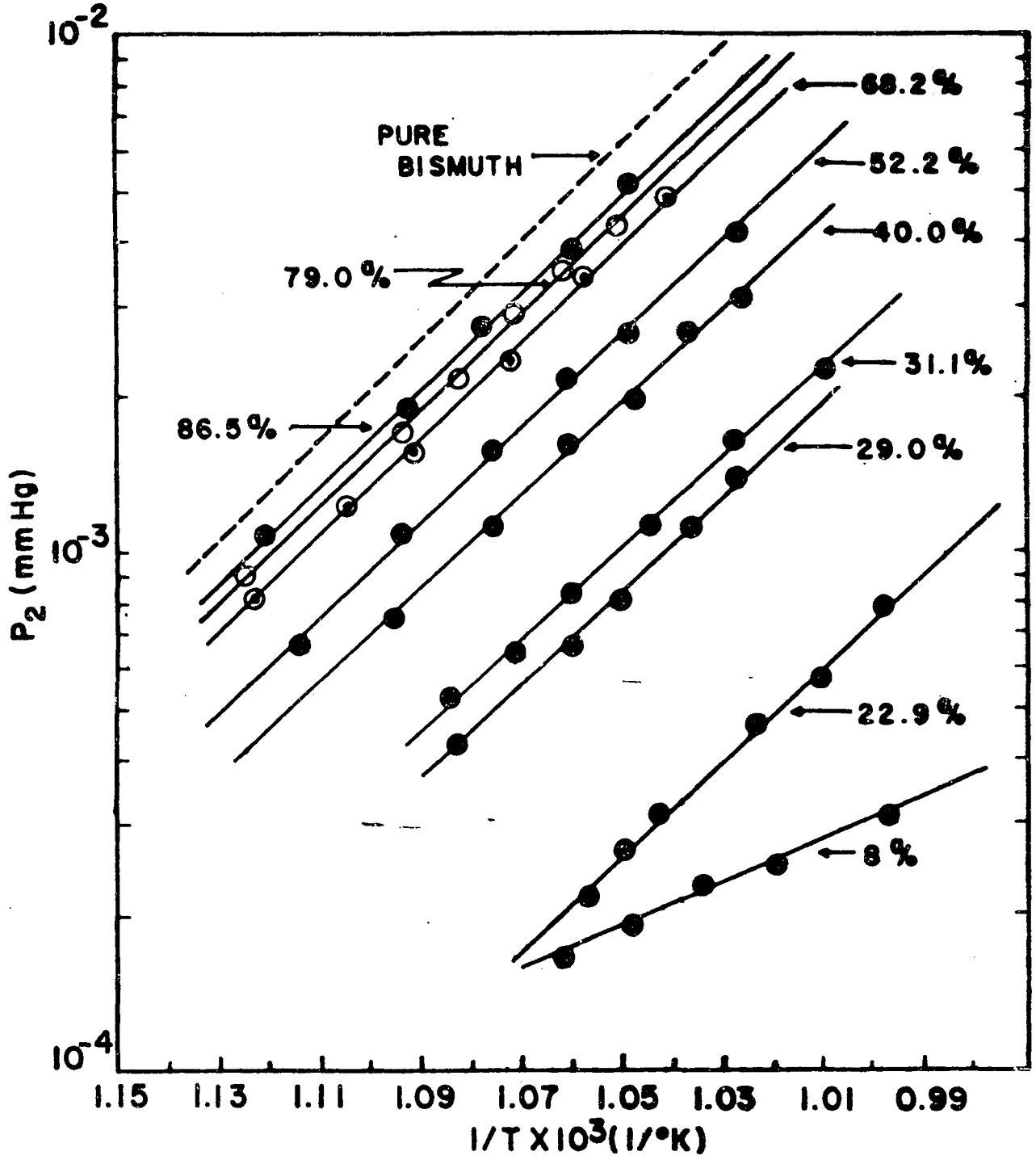

Fig. 12— Diatomic Pressure of Bismuth in Equilibrium with Silver-Bismuth Alloys

and 1000°K are 1.207×10^{-7}, 6.125×10^{-7}, 6.125×10^{-6}, and 9.659×10^{-6}. Since total pressure of bismuth vapor is theoretically identical to the values of $(P_1 + P_2)$ where P_1, P_2 are the monatomic pressure and diatomic pressure of bismuth, both the monatomic pressure of bismuth and the diatomic pressure of bismuth can be calculated by solving Equation 7 with the above relationship at a given temperature. Those results at 850°K, 900°K, 950°K, and 1000°K are summarized in Table VII.

TABLE VII

THERMODYNAMIC ACTIVITIES OF BISMUTH IN THE SILVER-BISMUTH SYSTEM

Top	Value from Monatomic Vapor Pressure
Middle	Value from Diatomic Vapor Pressure
Bottom	Value from Equilibrium Constant

Alloy Composition (N_{Bi})	850°K	900°K	950°K	1000°K
0.865	0.895	0.896	0.896	0.892
	0.910	0.905	0.901	0.896
	0.910	0.903	0.900	0.896
0.790	0.841	0.846	0.849	0.853
	0.866	0.861	0.851	0.853
	0.859	0.857	0.855	0.851
0.682	0.813	0.803	0.793	0.784
	0.812	0.810	0.800	0.791
	0.818	0.808	0.798	0.787
0.522	0.656	0.654	0.651	0.650
	0.685	0.672	0.661	0.651
	0.675	0.667	0.658	0.650

TABLE VII--(Continued)

Alloy Composition (N_{Bi})	850°K	900°K	950°K	1000°K
0.400	0.612	0.582	0.557	0.535
	0.612	0.588	0.568	0.551
	0.610	0.586	0.563	0.544
0.311	0.442	0.424	0.409	0.396
	0.451	0.430	0.408	0.311
	0.444	0.427	0.411	0.396
0.290	0.360	0.391	0.374	0.360
	0.370	0.379	0.375	0.370
	0.366	0.384	0.374	0.366
0.229	--	0.209	0.205	0.202
		0.210	0.207	0.202
		0.209	0.205	0.202
0.080	--	0.256	0.178	--
		0.258	0.180	
		0.250	0.179	

From the knowledge of thermodynamic activities of bismuth obtained from Equation 8, activities of silver were determined by integrating the Gibbs-Duhem equation with the alpha function (48) to the phase boundary of liquid alloy. A detailed illustration on the performance of Gibbs-Duhem integration is given in Appendix I.

The activity of silver at the phase boundary of liquid alloy is taken to be the mole fraction of silver at the solidus point (N_{Ag} = 0.980 at 950°K, N_{Ag} = 0.978 at 1000°K) under the equilibrium condition. This estimate is based upon the assumption that Raoult's law is obeyed by the

silver in the silver-rich primary solid solution. The activity of silver thus obtained is relative to pure solid silver at 950°K. Thence the activities of silver relative to the supercooled liquid of pure silver are calculated from the activity of silver relative to the pure solid silver by the utilization of available thermodynamic data of silver metal (49). The value of $\ln a^*_{Ag}$, where a^*_{Ag} is activity of silver at the phase boundary (N_{Ag} = 0.787 at 950°K, N_{Ag} = 0.818 at 1000°K) is respectively calculated to be -0.372, -0.296. Results of activities at 950°K are graphically shown in Figure 13 and summarized in Table VIII. Also results of activities at 1000°K are summarized in Table IX.

In Figure 13, the dotted line indicates the activity in the supercooled region of the alloy. The method of determining activities in this region is elucidated in Appendix I.

The partial molar entropy of any constituent is given by the following equation:

$$\Delta\bar{S}_i = -\frac{d\Delta F_i}{dT} \qquad (30)$$

Although the partial molar entropy is generally dependent on temperature, a simplifying assumption is made that the partial molar entropy is independent of temperature in the temperature range employed. Hence, the partial molar entropy is calculated from the Clasius-Clapeyron equation of vapor pressure. In such a manner, the partial molar entropies were evaluated, respectively, from monatomic vapor pressure and from diatomic vapor pressure. Agreement between these separately calculated

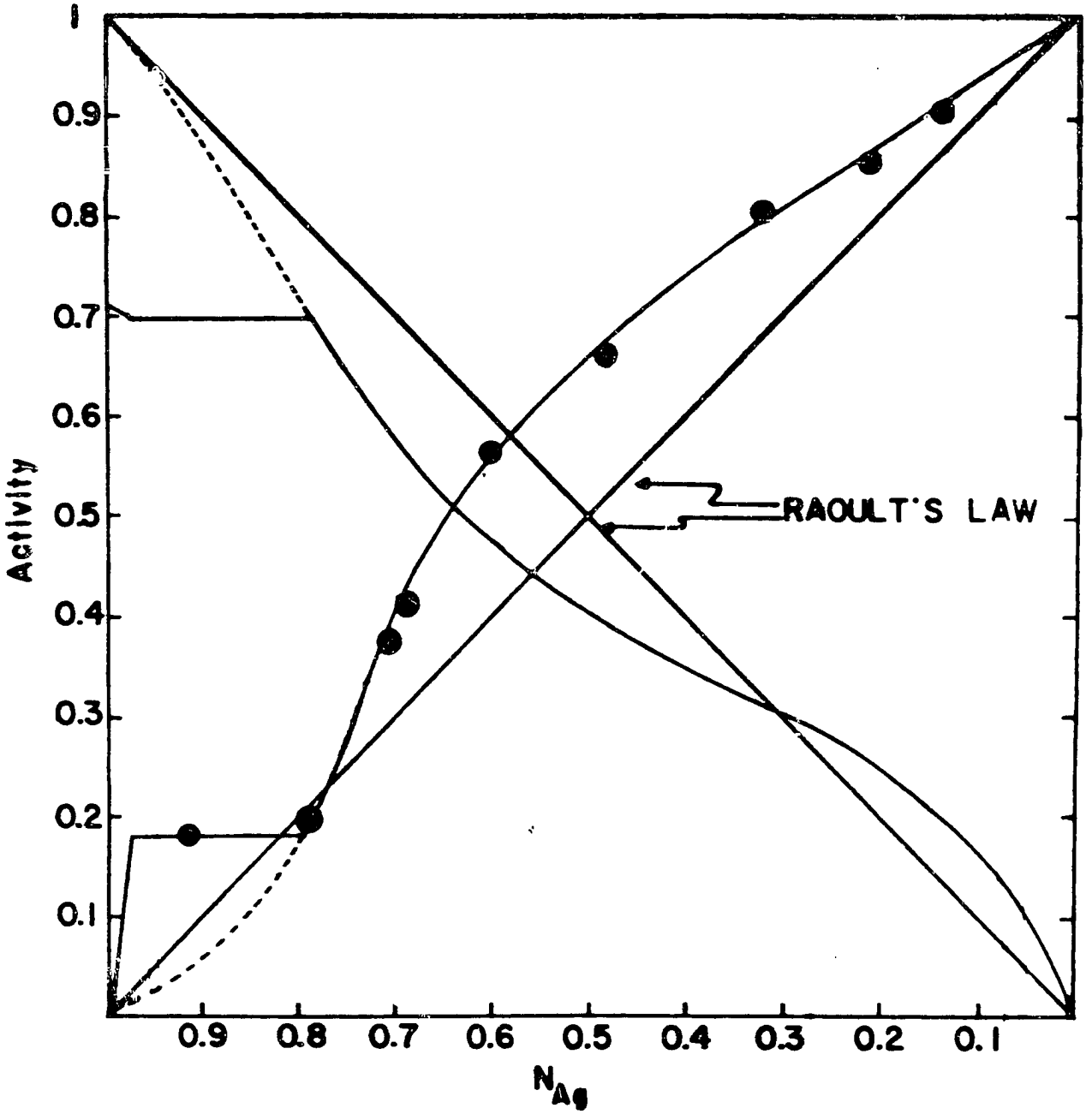

Fig. 13– Activities of Bismuth and Silver in the Ag-Bi Liquid Alloys at 950°K

values is very poor. These disagreements are probably caused by uncertainties in temperature coefficients of the vapor pressure equation.

TABLE VIII

THERMODYNAMIC ACTIVITIES OF SILVER AND BISMUTH AT 950°K

Alloy Composition N_{Ag}	a_{Ag}	a_{Bi}
1*	1	0
0.9*	0.87_1	0.05_9
0.8*	0.71_8	0.17_9
0.787**	0.69_0	0.20_0
0.7	0.56_4	0.36_5
0.6	0.47_2	0.53_8
0.5	0.40_0	0.65_8
0.4	0.34_2	0.75_1
0.3	0.30_5	0.81_2
0.2	0.24_6	0.86_3
0.1	0.16_8	0.92_0
0	0	1

*Supercooled region

**Phase boundary

TABLE IX

THERMODYNAMIC ACTIVITIES OF SILVER AND BISMUTH AT 1000°K

Alloy Composition N_{Ag}	a_{Ag}	a_{Bi}
1*	1	0
0.9*	0.87_0	0.05_5
0.818**	0.74_4	0.14_8
0.8	0.71_4	0.17_8
0.7	0.56_7	0.35_6
0.6	0.46_3	0.52_4
0.5	0.38_7	0.65_0
0.4	0.33_4	0.73_3
0.3	0.28_1	0.80_5
0.2	0.23_1	0.86_0
0.1	0.15_4	0.91_9
0	0	1

*Supercooled region

**Phase boundary

Alternatively, the partial molar entropies of bismuth were calculated from a difference of two free energies between 900°K and 950°K. Free energies used in this calculation were determined by utilizing both

the equilibrium constant of bismuth vapor and the measured total pressure of alloy. The comparison of these results is summarized in Table X. The smoothed curve of partial molar entropies calculated in the latter manner was drawn and the partial molar entropy of silver was determined by integrating Gibbs-Duhem equation with the alpha function.

Since the solid solubility of silver is very limited, the activities of silver in the range of silver-rich primary solid solution can be assumed to follow the Raoult's law. The available thermodynamic data of silver metal and the phase diagram of the system make it possible to estimate the activities of silver at any point along the silver branch of liquidus. Activities of silver thus estimated were used to determine the partial entropy of bismuth by combination with the derived activities of silver at 950°K from the activities of bismuth. The comparison of results between the smoothed value of $\Delta\bar{S}_{Ag}$ from phase diagram is summarized in Table XI.

Thus, the partial quantities of silver and bismuth were used to compute the integral molar quantities for the liquid alloy at 950°K.

From the thermodynamic relationship $\Delta H = \Delta F + T\Delta S$, the integral molar enthalpy of liquid alloys can be calculated from a summation of ΔF and $T\Delta S$. Thermodynamic properties of silver-bismuth system are summarized in Table XII. These calculated values are based on the standard state of supercooled liquid silver and of liquid bismuth at the corresponding temperature.

TABLE X

PARTIAL MOLAR ENTROPIES OF BISMUTH

Alloy Composition N_{Bi}	ΔS_{Bi}(cal/gmol°K) from monatomic pressure	ΔS_{Bi}(cal/gmol°K) from diatomic pressure	ΔS_{Bi}(cal/gmol°K) from total press. and Equil. Const.	ΔS_{Bi}(cal/gmol°K) smoothed value
0.865	0.207	0.356	0.336	0.29
0.790	0.159	0.475	0.436	0.49
0.682	0.898	0.902	0.936	0.81
0.522	0.967	1.426	1.314	1.57
0.400	2.776	2.381	2.780	2.33
0.311	3.086	3.247	3.136	3.08
0.290	3.475	2.379	2.826	3.30
0.229	3.875	3.715	3.810	4.00

TABLE XI

THE PARTIAL ENTROPY OF SILVER AT 950°K

Alloy Composition N_{Ag}	The Smoothed Value ΔS_{Ag}(cal/gmol°K)	The Calculated Value ΔS_{Ag}(cal/gmol°K)
0.787	0.616	--
0.7	0.97	1.20
0.6	1.42	1.55
0.5	1.98	2.26
0.4	2.59	2.84
0.3	3.32	3.13
0.2	4.24	4.15
0.1	5.69	5.46

Discussion

Lead Vapor Pressure

A comparison of previously reported vapor pressures of lead with those determined in this study is graphically shown in Figure 14. It has been pointed out that there is some evidence that values reported by Egerton (13) are lower than they should be. Introduction of a proper transmission coefficient may uniformly raise the vapor pressure data reported by Egerton, but such a correction was not made because of

limited data on the geometry of Egerton's effusion orifice.

TABLE XII

THERMODYNAMIC PROPERTIES OF THE SILVER-BISMUTH SYSTEM AT 950°K

Alloy Composition N_{Ag}	ΔF (cal/gmol)	ΔS (cal/gmol°K)	ΔH (cal/gmol)
0.9*	-770.9	0.8495	36.1
0.8*	-1148.5	1.3366	121.3
0.787**	-1199.1	1.382	113.8
0.7	-1327.1	1.603	195.7
0.6	-1320.4	1.780	370.6
0.5	-1260.9	1.870	515.1
0.4	-1135.2	1.732	510.2
0.3	-949.6	1.585	556.2
0.2	-752.1	1.216	403.1
0.1	-478.5	0.758	241.6

*Supercooled region

**Phase boundary

If free energy functions are available, the third law method yields the average value of determined standard heats of vaporization. Some investigators claim the preference of their data ascertaining that no trend of ΔH_{298} from individual vapor pressure points is observed with temperature.

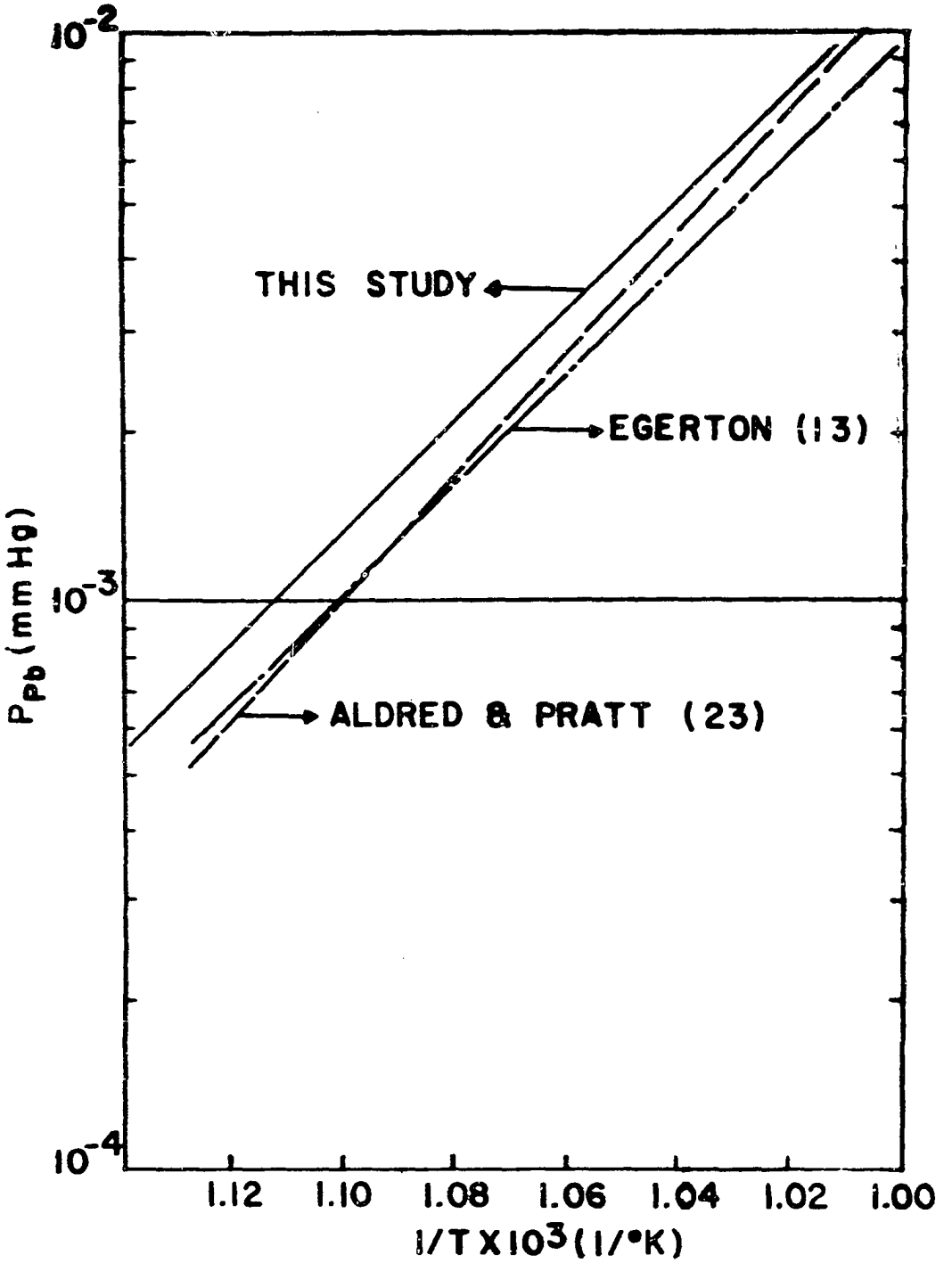

Fig. 14 – Vapor Pressure of Lead vs Reciprocal Temperature

Although this test is considered to be theoretically sound, such a test is rather insensitive, especially in the case where two different investigations report ΔH_{298} values differing by one or two kcal with very low error limit. An alternative method was proposed by Herrick (50). The comparison of ΔH_{298} from the third law method and the second law method (or slope method) may provide a sensitive test of the consistency in the measured vapor pressure data. When the vapor pressure data are plotted on a logarithmic scale versus 1/T, the data lie upon a straight line, corresponding to a constant heat of vaporization over a range of experimental temperatures. At the same time the corresponding entropy can be estimated from the intercept of the straight line. A comparison of the results obtained in this study to those of previous investigators is shown in Table XIII.

Reasonable agreement exists on the third law values for the vaporization heat of lead. Aldred and Pratt's results show a large difference between the second law and the third law values indicating a significant temperature dependent error. The results of Egerton and this study show a much smaller difference. The comparisons of entropy for the vaporization at a given temperature in the experimental range are also shown in Table XIII. Hultgren's tabulation on the entropy is based upon both the spectroscopic data and experimental heat capacities; this method is considered to be more precise in determining the entropy than any other equilibrium method. A close agreement between the entropy

TABLE XIII

ENTHALPY AND ENTROPY OF VAPORIZATION OF LEAD

Author	Range of Temperature (^{o}K)	ΔH^{o}_{298}(2nd law) (kcal/g-mol)	ΔH^{o}_{298}(3rd law) (kcal/g-mol)	$\Delta S_{900}{}^{o}$K (cal/g-mol. deg)
Present study	875-975	47.01	46.60	22.8
Aldred and Pratt (23)	880-1050	51.78	46.81	27.3
Egerton (13)	800-1050	48.78	47.17	23.0
Hultgren (15)			46.60	22.38

value listed by Hultgren and the value obtained from this present study is noted.

Bismuth Vapor Pressure

Figure 9 shows the standard heats of vaporization by the third law method for each experimental determination. There seems to exist a small temperature dependence in the monomer and dimer value. However, the heat of dissociation at 298^{o}K does not show any discerible trend with temperature.

A comparison of previously reported vapor pressure of bismuth with those determined in this study is graphically shown in Figure 15.

The standard heats of vaporization for monomeric bismuth vapor and dimeric bismuth vapor were calculated by both the second law method and the third law method; those calculations were based on Stull and Sinke's data of bismuth vapors and liquid. These results are summarized in Table XIV.

The third law values for bismuth show reasonable agreement among these works, but the second law values exhibit large variations. Agreements between the second law values and the third law values in previously reported works are extremely poor, and temperature dependent errors are apparent in those works. Approximately 3.5% deviation of the second law value from the third law value was found in this study. This indicates a slight temperature dependent error in the diatomic pressure data and monomeric pressure data.

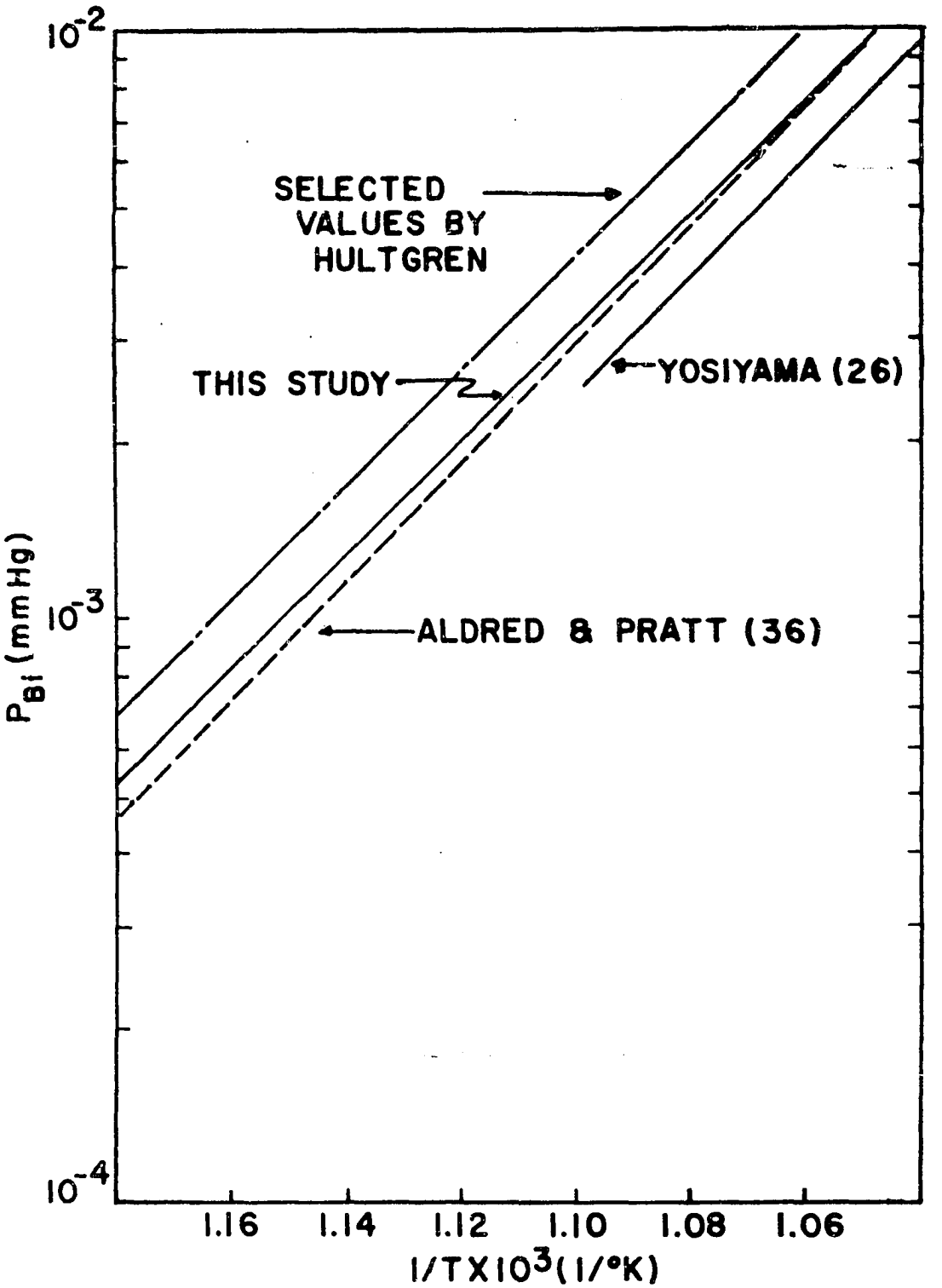

Fig. 15 — Vapor Pressure of Bismuth vs Reciprocal Temperature

TABLE XIV

HEAT OF VAPORIZATION OF BISMUTH

Author	Range of Temperature (°K)		ΔH^{o}_{298}(3rd law) (kcal/g-atom)	ΔH^{o}_{298}(2nd law) (kcal/g-atom)
Present study	850-950	Monomer	50.18	49.86
		Dimer	52.83	51.00
Aldred and Pratt (36)	824-970	Monomer	50.13	56.39
		Dimer	52.72	52.15
Yosiyama (26)	913-971	Monomer	50.05	59.68
		Dimer	53.24	49.40
Ko (25)	1100-1220	Monomer	47.50	60.30
		Dimer	55.30	44.08

As previously mentioned, the B coefficient in the vapor pressure, which is determined from the least squares treatment of Control Condition One, is highly insignificant. Since it is apparent that the linear effect of temperature as measured by log T may be insignificant at the 95% confidence level, the determination of A, B and C coefficients by correlating vapor pressure data with the three-parameter equation is impractical in most cases of the experimental technique. In order to obtain physically significant A, B and C coefficients by correlating the vapor pressure data with the three-parameter equation, it is required to employ the wide range of experimental temperature. Therefore, in most cases, the

application of the three-parameter equation to determine A and C coefficients seems to be favorable, because B coefficient may be accurately obtained from the available thermodynamic data.

The Silver-Bismuth Alloy

Activities of both bismuth and silver previously reported are shown in Table XV. Activities of bismuth at 1000°K in this study were

TABLE XV

COMPARISON OF THERMODYNAMIC ACTIVITIES AT 950°K AND AT 1000°K

	950°K				1000°K			
	This Study		Gregorczyk (43, 44)		This Study		Aldred & Pratt (45)	
Alley N_{Ag}	a_{Bi}	a_{Ag}	a_{Bi}	a_{Ag}	a_{Bi}	a_{Ag}	a_{Bi}	a_{Ag}
0.8	--	--	--	--	0.18	0.71	0.17	0.72
0.7	0.37	0.56	0.49	0.61	0.36	0.57	0.36	0.56
0.6	0.54	0.47	0.65	0.52	0.53	0.46	0.54	0.47
0.5	0.66	0.40	0.75	0.47	0.65	0.39	0.65	0.39
0.4	0.75	0.34	0.82	0.42	0.73	0.34	0.75	0.34
0.3	0.81	0.31	0.87	0.38	0.81	0.28	0.84	0.27
0.2	0.86	0.25	0.93	0.31	0.86	0.23	0.90	0.21
0.1	0.92	0.17	0.97	0.22	0.92	0.15	0.93	0.16

calculated from the extrapolated pressure values beyond the experimental temperature range. Activities of silver were computed from the Gibbs-Duhem integration with the alpha function. A reasonable agreement between activity values of the present study and Aldred and Pratt's values is exhibited, but discrepancies between Gregorczyk's activities and the values of the present study are clearly shown. The deviation of the activities of bismuth from the ideal law is observed to be positive in the bismuth rich solution, as in Aldred and Pratt's investigation, negative deviation from ideal law is observed in the silver rich solution.

The molal entropy of liquid solution shows that the solution does not behave as a regular solution and that a slight positive excess value is found as in previously reported results.

The molal enthalpy of liquid solution shows its maximum (approximately 550 cal/mol) at 30 atomic percent bismuth, this value is very high in comparison with the results by the calorimetric method, and also a plateau which is observed in the Kleppa's results (46) is not shown in the present study. Despite the fact that uncertainties in thermal quantities obtained from the temperature coefficient of the vapor pressure are certainly higher than the activity, the definite qualitative trend and magnitude of enthalpy values are in reasonable agreement with the results of the calorimetric method.

The uncertainties of activities are estimated to be 5% to 7% of the measured values by assuming that all errors in the activities occur

in the measurement of alloy vapor pressures. By applying the same assumption, the uncertainties of partial entropies of bismuth are estimated to be 1 to 2 cal/g mole.

A comparison of enthalpy results previously reported is graphically shown in Figure 16 and also the comparison of thermodynamic properties is given in Table XVI.

A retrograde solubility of bismuth occurs in the silver rich solution. The value of partial molar entropy of bismuth needed for the appearance of this phenomenon may be large (51). A large disparity of atom size as well as the valence difference between components maybe responsible for such a phenomenon. It is well-known that every configurational factor which reflects in the enthalpy will also affect the excess entropy of the solution. Therefore, the larger positive (or negative) enthalpy which is attributed to nonconfigurational factors, the larger positive (negative) is the excess entropy. Conjectures on the various sources of nonconfigurational factors have been made in textbooks on the statistical thermodynamics, but to this writer's knowledge no theoretical justification can be found in the literature. In the silver-bismuth liquid system, the partial free energy of components are found to be inflected. The characteristics of inflection phenomena can be explained only by the fact that two nonconfigurational factors contribute to the excess thermodynamic quantities in the opposing directions. In other words, the positive contribution to the excess thermodynamic quantities from one

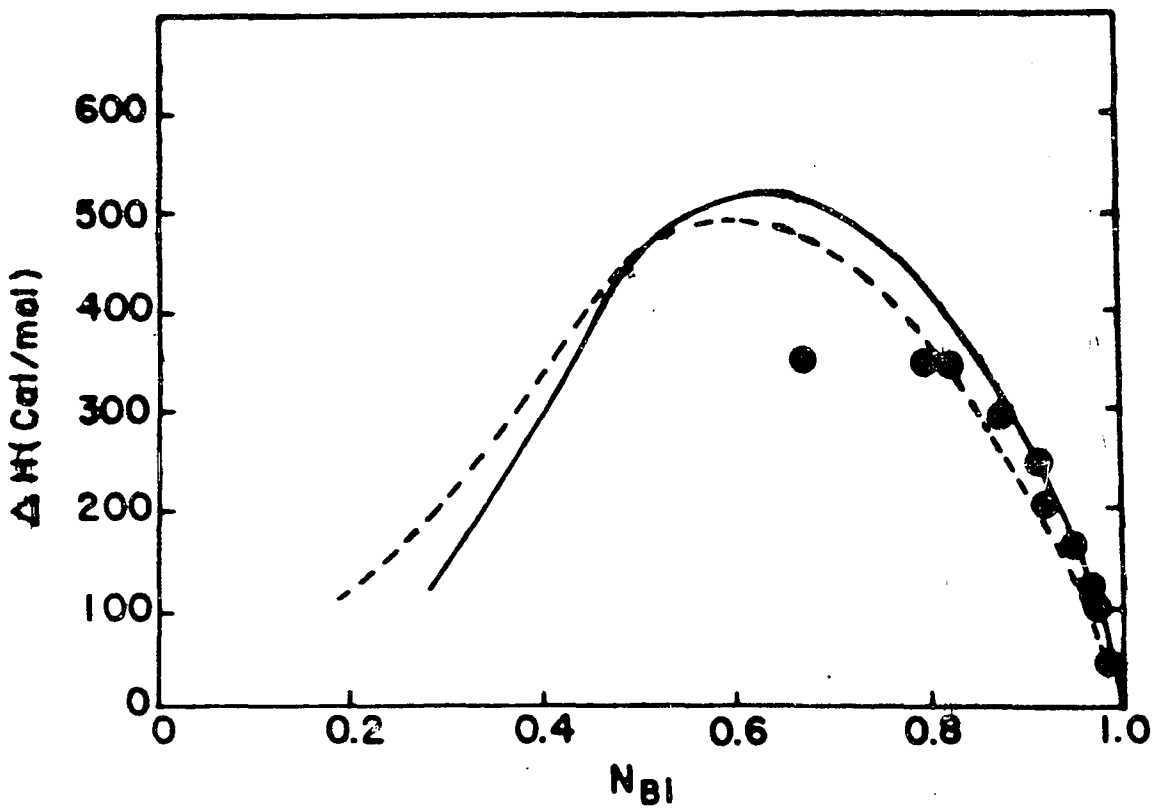

Fig. 16— The Comparison of Molal Enthalpies

Legend ———— Present Study

- - - - - - - - Pratt and Aldred (45)

● ● ● ● ● Kleppa (46)

TABLE XVI

COMPARISON OF THERMODYNAMIC PROPERTIES AT 1000°K

Alloy Composition N_{Ag}	This Study			Aldred and Pratt		
	ΔF(cal/mole)	ΔS(cal/mol. deg)	ΔH(cal/mole)	ΔF(cal/mole)	ΔS(cal/mol. deg)	ΔH(cal/mole)
0.9*	-826.8	0.84	13	-875	--	
0.818**	-1171.6	--	--	--	--	
0.8	-1226.4	1.33	110	-1240	1.37	120
0.7	-1405.3	1.60	198	-1410	1.63	220
0.6	-1432.4	1.780	348	-1450	1.79	340
0.5	-1371.4	1.87	509	-1385	1.85	460
0.4	-1243.1	1.73	489	-1250	1.76	500
0.3	-1060.3	1.58	525	-1040	1.51	460
0.2	-822.4	1.21	386	-795	1.12	330
0.1	-540.7	0.75	217	-470	0.67	200

*Supercooled region

**Phase boundary

nonconfigurational factor prevails in a limited range of composition, in turn, it is gradually counterbalanced by the other nonconfigurational factor which contributes to negative excess quantities.

CHAPTER IV

CONCLUSIONS

1. A torsion-Knudsen Effusion-Recoil apparatus with an automatic controlling and microbalance system was devised which permits the equilibrium study of two species vapor with both convenience and precision. In many substances, e.g., sulfur, selenium, sodium, sulfides, chlorides, it has been proved that vapors under equilibrium consist of two species in a certain interval of temperatures. The application of this technique to such substances is suitable.

2. The average molecular weight of lead was determined to be 207 ± 2.27, in the range of temperature $870^{\circ}K$ to $980^{\circ}K$. The molecular weight of lead determined is monatomic. The heat of vaporization of lead by the third law method was determined to be 46.00 ± 0.02 kcal/g-atom at $298^{\circ}K$. The best correlation of the experimental data on lead is given by the following equation:

$$\log P(atm) = (-10,186 \pm 119)/T - 1.1071 \log T + (8.738 \pm 0.123)$$

3. The average molecular weight of bismuth was determined

as the function of temperature assuming the presence of a monomer and dimer species. The bismuth vapor composition is approximately 65 per cent Bi_2 and 35 per cent Bi in the temperature range of investigation, 850°K to 950°K. The correlation of experimentally determined molecular weights as a function of temperature is given by the following equation:

$$\log M = (93.611 \pm 3.546)/T + (2.433 \pm 0.039)$$

The following equation represents the observed total vapor pressure of bismuth in the temperature range, 850°K to 950°K:

$$\log P(atm) = (5.24 \pm 0.24) - (9,656 \pm 218)/T$$

The average heats of vaporization of the bismuth species by the third law method were determined to be:

$$\Delta H^{o}_{298} = 50.18 \pm 0.07 \text{ kcal/g-atom} \quad \text{for the monomer}$$

$$\Delta H^{o}_{298} = 52.83 \pm 0.09 \text{ kcal/g-mole} \quad \text{for the dimer}$$

The equilibrium constant as the function of temperature is given by the following equation:

$$\log K(atm) = (5.766 \pm 0.439) + (-10,782 \pm 396)/T$$

4. The measured activity coefficient of bismuth at 950°K is greater than one in the bismuth rich solution and less than one in the silver rich solution; the inflection point of the activity coefficient occurs

at $N_{Bi} = 0.23$. The activity coefficient of silver (relative to the supercooled liquid of silver) is greater than one in the bismuth rich solution and less than one in the silver rich solution and shows an inflection point at $N_{Bi} = 0.7$. The entropy of the liquid solution does not follow the regular solution model; it exhibits a slight positive excess entropy. The enthalpy of the liquid solution exhibits a maximum (approximately 550 kcal/g-mole) at $N_{Bi} = 0.6$.

BIBLIOGRAPHY

1. Margrave, J. L. "Physicochemical Measurements at High Temperature." Edited by Bockris, et al., Butterworths Scientific Publication Ltd., London (1959).

2. Freeman, R. D. "Momentum Sensors." Oklahoma State University, Stillwater, Oklahoma (1964).

3. Volmer, M. Z. Phys. Chem. Boden. Fest, 863 (1931).

4. Searcy, A. W. and Freeman, R. D. J. Chem. Phys., 23, 88 (1955).

5. Clausing, P. Z. Phys. Chem., 66, 471 (1930).

6. Aldred, A. T. and Pratt, J. N. Rev. Scientific Inst., 36, 465 (1959).

7. Rosenblatt, G. M. and Birchnall, C. E. J. Chem. Phys., 35, 788 (1961).

8. Myles, K. M. Argonne National Lab. Report 6675 (Feb., 1963).

9. Munier, Z. A. and Searcy, A. W. J. Electrochem. Soc., 111, 1170 (1964).

10. Newmann, K. and Volker, E. Z. Phys. Chem., A161, 33 (1932).

11. Bell, M. and Hultgren, R. "Heat Capacity of Liquid Bismuth." N P-9146 (1960).

12. Mayer, H. R. Z. Phys. Chem., 67, 240 (1931).

13. Egerton, A. C. Phil. Mag., 33, 33 (1917).

14. Ernsberger, F. M. and Pitman, H. W. Rev. of Scientific Inst., 26, 584 (1955).

15. Hultgren, R., Orr, R. L. and Kelly, K. K. "The Selected Values of Thermodynamic Properties of Metals and Alloys." John Wiley and Sons, New York (1964).

16. Busey, R. H. and Giaque, W. F. J. Am. Chem. Soc., 75, 806 (1953).

17. Rodebush, W. H. and Dixon, A. L. Phys. Rev., 26, 851 (1925).

18. Rodebush, W. H. J. Am. Chem. Soc., 47, 1036 (1925).

19. Harteck, P. Z. Phys. Chem., 134, 1 (1928).

20. Bauer, E. and Brunner, R. Helv. Chim. Acta., 27, 958 (1934).

21. Granovskaya, A. P. and Lubmiov, A. P. Zuhr. Fis. Khim., 27, 1437 (1953).

22. Ingold, C. K. J. Chem. Soc., 121, 2419 (1922).

23. Aldred, A. T. and Pratt, J. N. Trans. Faraday Soc., 57, 611 (1961).

24. Stull, D. R. and Sinke, G. C. "Thermodynamic Properties of Elements." Am. Chem. Soc., Washington, D.C., (1956).

25. Ko, C. C. J. Franklin Inst., 217, 173 (1934).

26. Yosiyama, M. J. Chem. Soc. Japan, 62, 204 (1941).

27. Miller, R. C. and Kush, P. J. Chem. Phys., 25, 860 (1956).

28. Granovskaya, A. and Lubmiov, A. J. Phys. Chem. U.S.S.R., 22, 103 (1948).

29. Martinkevich, G. M. Moscow University Scientific Journal, 5, 67 (1958).

30. O'Donnell, T. A. Australian J. of Science, A-8, 493 (1955).

31. Brackett, E. and Brewer, L. Univ. Calif. Radiation Lab. Report 3712, 5PP (1957).

32. Almy, G. M. and Sparks, F. M. Phys. Rev., 44, 365 (1933).

33. Cosgarea, A. C., Jr. Doctoral Dissertation: "Some Properties of Uranium-Bismuth Alloys." Univ. of Michigan, (1959).

34. Rice, P., Ragone, D. and Craig, J. U.S. Atomic Energy Commission T.I.D. - 17348 (1964).

35. Denison, G. Doctoral Dissertation: "A Study of the Vapor Atomicity of Some Metals." University of Oklahoma, (1962).

36. Aldred, A. T. and Pratt, J. N. J. Chem. Phys., 38, 1085 (1963).

37. Leu, A. Z. f. Phys., 49, 304 (1928).

38. Heycock, C. T. and Neville, F. H. Phil. Trans. Roy. Soc. (London) A 189, 46 (1897).

39. Petrenco, G. I. Z. Anorg. Chem., 50, 136 (1906).

40. Nathans, M. W. and Leider, M. J. of Phys. Chem., 66, 2012 (1916).

41. Kleppa, O. J. J. Phys. Chem., 60, 446 (1956).

42. Bonnier, E. and Desre, P. Compt. Rend., 249, 1664 (1959).

43. Gregorczyk, Z. Roczniki Chem., 35, 307 (1961).

44. Gregorczyk, Z. Roczniki Chem., 34, 621 (1960).

45. Aldred, A. T. and Pratt, J. N. Trans. Faraday Soc., 58, 673 (1962).

46. Kleppa, O. J. J. Phys. Chem., 521, 65 (1959).

47. Lumsden. "Thermodynamics of Alloys." Inst. of Metals, London (1952).

48. Darken, L. S. and Gurry, R. W. "Physical Chemistry of Metals." McGraw-Hill, New York (1953).

49. Wicks, C. E. and Block, F. E. "Thermodynamic Properties of 65 Elements," Bureau of Mines Bulletin, 605, Washington D.C. (1960).

50. Herrick, C. C. Trans. Am. Inst. Met. Min. Eng., 230, 1439 (1964).

51. Swalin, R. A. "Thermodynamics of Solids," John Wiley and Sons, New York (1961).

52. Kennard, E. H. "Kinetic Theory of Gases." McGraw-Hill, New York (1938).

APPENDIX A

CELL CONSTANTS

Cell A

$a_1 = 3.173 \times 10^{-3}\ cm^2$	$q_1 = .53$ cm	$f_1 = .779$	$k_1 = .717$
$a_2 = 3.041 \times 10^{-3}\ cm^2$	$q_2 = .50$ cm	$f_2 = .776$	$k_2 = .713$

Cell B

$a_1 = .005340\ cm^2$	$q_1 = .483$ cm	$f_1 = .7537$	$k_1 = .6880$
$a_2 = .006420\ cm^2$	$q_2 = .478$ cm	$f_2 = .7709$	$k_2 = .7073$

Cell C

$a_1 = .007628\ cm^2$	$q_1 = .445$ cm	$f_1 = .7611$	$k_1 = .6962$
$a_2 = .008928\ cm^2$	$q_2 = .430$ cm	$f_2 = .7675$	$k_2 = .7032$

APPENDIX B

LEAD RESULTS

Temp. (^{o}K)	Cell	G (grams/sec)	P (atm.)	H^{o}_{298} (kcal/g-atom)	M = M_1
876.6	C	1.750×10^{-7}	7.024×10^{-7}	46.60	204.9
876.7	B	--	7.264	46.58	-
887.2	B	--	9.415	46.64	-
892.8	C	2.776	1.122×10^{-6}	46.62	206.0
898.7	B	2.336	1.345	46.58	203.2
909.0	C	4.271	1.719	46.64	211.4
920.5	C	5.943	2.442	46.57	205.3
923.0	B	4.546	2.608	46.57	210.0
934.5	C	8.419	3.426	46.62	212.4
943.0	B	7.269	4.302	46.60	201.7
950.0	C	1.242×10^{-6}	5.133	46.60	209.3
960.7	B	1.140	6.693	46.60	208.6
974.5	B	1.568	9.273	46.61	208.6
			Average	46.60	207.4

APPENDIX C

BISMUTH RESULTS

Temp. (°K)	Cell	G (grams/sec)	P_1 (atm.)	P_2 (atm.)	H^o_{2981} (kcal) (g-atom)	H^o_{2982} (kcal) (g-mole)	D^o_{298} (kcal) (g-mole)	M	M_1
848.7	C	2.333×10^{-7}	2.312×10^{-7}	4.818×10^{-7}	50.20	52.73	46.67	342.4	350.2
861.7		3.599	3.703	7.411	50.09	52.67	47.51	340.4	348.4
870.0		4.588	4.826	9.433	50.07	52.66	47.48	339.2	347.3
872.2	B	3.370	5.011	9.787	50.13	52.69	47.57	339.2	347.2
896.5		6.270	9.688	1.829×10^{-6}	50.23	52.76	47.70	337.5	345.6
916.5		1.087×10^{-6}	1.767×10^{-6}	3.154	50.26	52.97	47.55	334.7	343.0
917.7		1.204	1.971	3.489	50.11	52.84	47.38	334.3	342.6
933.2		1.669	2.766	4.870	50.28	52.97	47.59	334.0	342.3
937.7		1.976	3.326	5.749	50.17	52.90	47.44	333.1	341.4
943.8		2.182	3.698	6.357	50.27	53.00	47.54	332.8	341.1
953.7		2.839	4.907	8.266	50.22	52.98	47.46	331.8	340.1
				Average	50.18	52.83	47.46		

APPENDIX D

X_{Bi} = 0.865 ALLOY

Cell B

Temp. (°K)	G	P	P_1	P_2	M	M_i
892.7	5.041×10^{-7}	2.259×10^{-6}	8.288×10^{-7}	1.430×10^{-6}	333.0	341.3
903.7	6.847×10^{-7}	3.093×10^{-6}	1.149×10^{-6}	1.943×10^{-6}	331.9	340.2
914.7	8.888×10^{-7}	4.047×10^{-6}	1.531×10^{-6}	2.516×10^{-6}	330.4	338.9
928.2	1.263×10^{-6}	5.808×10^{-6}	2.237×10^{-6}	3.570×10^{-6}	328.9	337.4
942.7	1.799×10^{-6}	8.348×10^{-6}	3.251×10^{-6}	5.096×10^{-6}	328.0	336.5
953.6	2.368×10^{-6}	1.107×10^{-5}	4.395×10^{-6}	6.680×10^{-6}	326.4	335.0

X_{Bi} = 0.79 ALLOY

Cell B

Temp. (°K)	G	P	P_1	P_2	M	M_i
889.2	4.200×10^{-7}	1.883×10^{-6}	7.022×10^{-7}	1.180×10^{-6}	329.8	339.4
914.4	8.117×10^{-7}	3.711×10^{-6}	1.451×10^{-6}	2.260×10^{-6}	327.7	336.2
923.2	1.017×10^{-6}	4.679×10^{-6}	1.845×10^{-6}	2.833×10^{-6}	326.9	335.5
933.7	1.324×10^{-6}	6.130×10^{-6}	2.431×10^{-6}	3.698×10^{-6}	326.5	335.0
941.7	1.618×10^{-6}	7.528×10^{-6}	3.007×10^{-6}	4.520×10^{-6}	325.8	334.4
951.5	2.070×10^{-6}	9.705×10^{-6}	3.950×10^{-6}	5.754×10^{-6}	324.2	332.9

X_{Bi} = 0.682 ALLOY

Cell B

Temp. (°K)	G	P	P_1	P_2	M	M_i
890.5	3.932×10^{-7}	1.775×10^{-6}	6.968×10^{-7}	1.078×10^{-6}	327.4	335.9
905.2	5.901×10^{-7}	2.689×10^{-6}	1.066×10^{-6}	1.623×10^{-6}	326.5	335.1
916.2	7.535×10^{-7}	3.469×10^{-6}	1.418×10^{-6}	2.051×10^{-6}	323.9	332.5
932.7	1.144×10^{-6}	5.323×10^{-6}	2.204×10^{-6}	3.119×10^{-6}	322.7	331.4
945.5	1.609×10^{-6}	7.554×10^{-6}	3.174×10^{-6}	4.380×10^{-6}	321.4	330.1
961.0	2.289×10^{-6}	1.085×10^{-5}	4.639×10^{-6}	6.220×10^{-6}	319.9	328.7

X_{Bi} = 0.522 ALLOY

Cell B

Temp. (°K)	G	P	P_1	P_2	M	M_i
897.6	3.442×10^{-7}	1.586×10^{-6}	7.034×10^{-7}	8.835×10^{-7}	316.5	325.3
914.4	5.301×10^{-7}	2.460×10^{-6}	1.073×10^{-6}	1.387×10^{-6}	318.0	326.8
929.6	7.987×10^{-7}	3.764×10^{-6}	1.721×10^{-6}	2.043×10^{-6}	313.5	322.4
943.0	1.108×10^{-6}	5.269×10^{-6}	2.437×10^{-6}	2.832×10^{-6}	312.4	321.3
953.2	1.378×10^{-6}	6.613×10^{-6}	3.129×10^{-6}	3.483×10^{-6}	310.1	319.0
972.7	2.168×10^{-6}	1.053×10^{-5}	5.069×10^{-6}	5.466×10^{-6}	308.4	317.4

X_{Bi} = 0.400 ALLOY

Cell B

Temp. (°K)	G	P	P_1	P_2	M	M_i
912.7	4.107×10^{-7}	1.936×10^{-6}	9.385×10^{-7}	9.978×10^{-7}	307.7	316.7
929.2	6.206×10^{-7}	2.957×10^{-6}	1.451×10^{-6}	1.506×10^{-6}	306.4	315.4
943.0	8.670×10^{-7}	4.167×10^{-6}	2.060×10^{-6}	2.106×10^{-6}	305.7	314.6
954.7	1.087×10^{-6}	5.295×10^{-6}	2.730×10^{-6}	2.565×10^{-6}	301.3	310.2
964.4	1.453×10^{-6}	7.109×10^{-6}	3.649×10^{-6}	3.460×10^{-6}	301.7	310.7
974.1	1.716×10^{-6}	8.439×10^{-6}	4.341×10^{-6}	4.097×10^{-6}	301.5	310.4

X_{Bi} = 0.311 ALLOY

Cell B

Temp. (°K)	G	P	P_1	P_2	M	M_i
922.2	3.229×10^{-7}	1.573×10^{-6}	8.881×10^{-7}	6.849×10^{-7}	291.1	300.0
933.0	4.067×10^{-7}	2.003×10^{-6}	1.160×10^{-6}	8.423×10^{-7}	288.1	296.8
943.0	5.292×10^{-7}	2.621×10^{-6}	1.522×10^{-6}	1.098×10^{-6}	287.8	296.5
956.5	7.220×10^{-7}	3.615×10^{-6}	2.139×10^{-6}	1.476×10^{-6}	285.6	294.3
973.3	1.053×10^{-6}	5.335×10^{-6}	3.202×10^{-6}	2.133×10^{-6}	283.9	292.5
989.5	1.499×10^{-6}	7.685×10^{-6}	4.684×10^{-6}	3.001×10^{-6}	282.0	290.6

X_{Bi} = 0.29 ALLOY

Cell B

Temp. (°K)	G	P	P_1	P_2	M	M_i
973.2	9.357×10^{-7}	4.770×10^{-6}	2.949×10^{-6}	1.820×10^{-6}	280.3	288.7
964.7	7.575×10^{-7}	3.843×10^{-6}	2.371×10^{-6}	1.472×10^{-6}	280.5	289.0
951.2	5.556×10^{-7}	2.795×10^{-6}	1.714×10^{-6}	1.081×10^{-6}	281.3	289.8
943.2	4.515×10^{-7}	2.258×10^{-6}	1.372×10^{-6}	8.885×10^{-7}	282.4	290.9
923.2	2.830×10^{-7}	1.398×10^{-6}	8.426×10^{-7}	5.556×10^{-7}	283.4	292.0

X_{Bi} = 0.229 ALLOY

Cell B

Temp. (°K)	G	P	P_1	P_2	M	M_i
946.0	2.097×10^{-7}	1.102×10^{-6}	8.145×10^{-7}	2.877×10^{-7}	256.6	263.5
959.0	2.948×10^{-7}	1.559×10^{-6}	1.150×10^{-6}	4.084×10^{-7}	256.8	263.7
977.4	4.512×10^{-7}	2.418×10^{-6}	1.812×10^{-6}	6.068×10^{-7}	254.6	261.4
989.0	5.718×10^{-7}	3.090×10^{-6}	2.334×10^{-6}	7.557×10^{-7}	253.4	260.1
1002.0	7.732×10^{-7}	4.205×10^{-6}	3.175×10^{-6}	1.029×10^{-6}	253.5	260.1

X_{Bi} = 0.080 ALLOY

Cell B

Temp. (°K)	G	P	P_1	P_2	M	M_i
941.5	1.685×10^{-7}	8.872×10^{-7}	6.650×10^{-7}	2.221×10^{-7}	254.6	261.3
953.5	2.066×10^{-7}	1.102×10^{-6}	8.466×10^{-7}	2.555×10^{-7}	251.0	257.4
967.2	2.559×10^{-7}	1.384×10^{-6}	1.088×10^{-6}	2.956×10^{-7}	247.6	253.6
980.0	3.112×10^{-7}	1.706×10^{-6}	1.375×10^{-6}	3.313×10^{-7}	243.9	249.5
1003.0	4.344×10^{-7}	2.431×10^{-6}	2.016×10^{-6}	4.147×10^{-7}	239.5	244.6

APPENDIX E

SILVER-BISMUTH PHASE DIAGRAM (15)

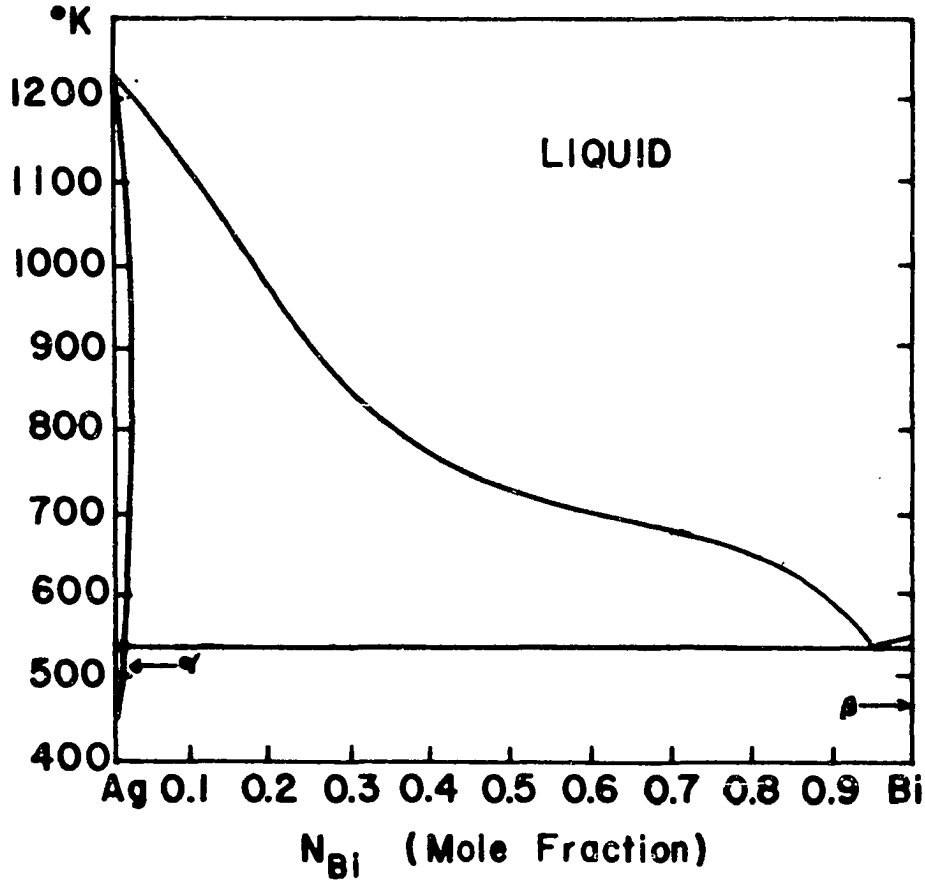

APPENDIX F

CHEMICAL ANALYSIS OF ALLOYS

Ten grams of KCNS was dissolved in 1000 ml of distilled water. This solution was then standardized against 25 ml of 0.1N $AgNO_3$ solution, using ferric ammonium sulfate as an indicator. The end point is characterized by a faint brown color adsorbed on the $FeCNS^{++}$ complex.

Two samples of each silver alloy were weighed out and dissolved in 15-20 ml of 1: 1 nitric acid solution. The oxides of nitrogen were then boiled out until the vapor above the solution was colorless. Titration was performed with KCNS as indicator $FeNH_4SO_4$ until faint brown colored end point is observed.

Several different compositions of silver-bismuth mixture (composition is determined by analytical balance) were prepared and chemically analyzed by the same manner. Results of chemical analysis are shown in Table A.

TABLE A

Sample	wt% of Ag	wt% of Ag (by titration)
No. 1	64.86	65.0
No. 2	36.97	37.23
No. 3	49.95	49.58
No. 4	95.67	96.35

Any conceivable interference due to bismuth ion was not observed in the wide range of alloy composition. The end point is fairly sharp and easily reproducible in most cases.

APPENDIX G

THE THIRD LAW METHOD AND THE SECOND LAW METHOD

The Third Law Method

By the application of the third law, the entropy change $\Delta S^{\circ}_{T} = S^{\circ}_{T}(g) - S^{\circ}_{T}(c)$ for the vaporization in their standard states at $T^{\circ}K$ is:

$$\Delta S^{\circ}_{T} = \int_{o}^{T} \Delta C_p \, d\ln T = \int_{o}^{298} \Delta C_p \, d\ln T + \int_{298}^{T} \Delta C_p \, d\ln T \qquad (1)$$

or

$$\Delta S^{\circ}_{T} = \Delta S^{\circ}_{298} + \int_{298}^{T} \Delta C_p \, d\ln T \qquad (2)$$

An enthalpy change for the vaporization is

$$\Delta H^{\circ}_{T} = \Delta H^{\circ}_{298} + \int_{298}^{T} \Delta C_p \, dT \qquad (3)$$

and the Free Energy Function (fef) is:

$$\frac{\Delta F^{\circ}_{T} - \Delta H^{\circ}_{298}}{T} = \frac{F^{\circ}_{T}(g) - H^{\circ}_{298}(g)}{T} - \frac{F^{\circ}_{T}(c) - H^{\circ}_{298}(c)}{T}$$

may be rewritten as:

$$\Delta H^{\circ}_{298} = T\left[\frac{F^{\circ}_{T}}{T} - \left(\frac{F^{\circ}_{T}(g) - H^{\circ}_{298}(g)}{T}\right) - \left(\frac{F^{\circ}_{T}(c) - H^{\circ}_{298}(c)}{T}\right)\right] \qquad (4)$$

In equation (4), the first term on the right is identical to (- R ln p) and also the second and third terms on the right is rearranged to

$$\frac{\Delta H_T - \Delta H^o_{298}}{T} - \Delta S^o_T = \frac{1}{T}\int_{298}^{T} \Delta C_p \, dT - \Delta S^o_{298} - \int_{298}^{T} \Delta C_p \, d\ln T \quad (5)$$

Those terms can be obtained from the standard tabulations which is based on spectroscopic and heat capacity data. Then the standard enthalpy change of vaporization may be calculated from each experimental vapor pressure.

The Second Law Method

If Δfef is nearly constant over the temperature range where the experimental vapor pressure has been measured, the vapor pressure data are correlated to

$$\log P(\text{atm}) = -\frac{A}{T} + C \quad (6)$$

Therefore, A (slope = $\frac{\Delta H^o_T}{4.5758}$. Since ΔH^o_T is regarded as an enthalpy of vaporization at the mean temperature of experiment measurements. From the experimentally determined ΔH^o_T, an enthalpy of vaporization at 298°K may be computed such as:

$$\Delta H^o_{298} = \Delta H^o_T - (H^o_T(g) - H^o_{298}(g)) + (H^o_T(c) - H^o_{298}(c))$$

In the same manner, the entropy of vaporization can be computed from an intercept of equation (6) such as

$$\Delta S^{o}_{298} = \Delta S^{o}_{T} - \left(S_T(g) - S_{298}(g)\right) - \left(S_T(c) - S_{298}(c)\right)$$

The second and third terms can be computed from the standard tabulations.

APPENDIX H

ERRORS IN EXPERIMENTAL MEASUREMENTS

The estimate of the maximum propagated errors in the experimental measurements is illustrated by the following examples:

(A) The maximum propagated error in the torque pressure measurement is:

$$\frac{\Delta P}{P} = \pm \frac{\Delta \beta}{\beta} \pm \frac{\Delta \alpha}{\alpha} + \frac{\Delta (a_1 q_1 f_1 + a_2 q_2 f_2)}{(a_1 q_1 f_1 + a_2 q_2 f_2)}$$

$$= 2.4\% \pm 5\% + 1.68\% = 9.08\%$$

(i) the maximum error due to the torsion constant can be estimated from the following relation.

$$\beta = \frac{2\pi^2 m r^2}{t^2}$$

thus

$$\frac{\Delta \beta}{\beta} = \pm 2\frac{\Delta r}{r} = \pm \frac{\Delta m}{m} \pm 2\frac{\Delta t}{t} = 2 \times 10^{-3} +$$

$$2 \times 10^{-3} + 2 \times 10^{-2} = 2.4\%$$

(ii) the maximum error due to the angle of deflection will occur

when reading the smallest angle of deflection which is 5 scale divisions; the scale can be read to one-half of a division, that is, the error in reading corresponds to one-fourth of a division.

(iii) the maximum error due to the area of the holes, perpendicular distance between the suspension point and holes, and orifice coefficient is

$$\frac{\Delta(a_1q_1f_1 + a_2q_2f_2)}{(a_1q_1f_1 + a_2q_2f_2)} = \frac{9.25 \times 10^{-5}}{5.5 \times 10^{-2}} = 1.68 \times 10^{-2} = 1.68\%$$

the estimated maximum errors of measurement for each cell dimension are:

$$\Delta a_1 = 1.0 \times 10^{-5}\ cm^2 \cong \Delta a_2$$

$$\Delta q_1 = 1.0 \times 10^{-3}\ cm \cong \Delta q_2$$

$$\Delta f_1 = 1.0 \times 10^{-2} \cong \Delta f_2$$

Since

$$\Delta(a_1q_1f_1 + a_2q_2f_2) = \left[(a_1f_1 + a_2f_2)\Delta a + (a_1f_1 - a_2f_2)\Delta q + (a_1q_1 + a_2q_2)\Delta f\right]$$

$$= (0.8) \times 10^{-5} + (9.5 \times 10^{-3}) \times 10^{-3} + (7.5 \times 10^{-3}) \times 10^{-2}$$

$$= 9.25 \times 10^{-5}$$

(B) The maximum propagated error for the molecular weight measurements,

$$\frac{\Delta M}{M} = \pm \frac{\Delta T}{T} \pm 2\frac{\Delta G/t}{G/t} \pm 2\frac{\Delta P}{P} \pm 2\frac{\Delta(a_1k_1 + a_2k_2)}{(a_1k_1 + a_2k_2)}$$

$$= (0.2\%) + (2 \times 2.98\%) + (2 \times 9.08\%) + (2 \times 1.61\%)$$

$$= 27.54\%$$

(i) the maximum error due to the temperature measurement

$$\frac{\Delta T}{T} = 0.2\%$$

(ii) the maximum error due to the mass effusion rate is

$$\frac{\Delta G/t}{G/t} = \pm \frac{\Delta G}{G} + \frac{\Delta t}{t} = 1.32\% + 1.66\% = 2.98\%$$

(iii) the maximum error due to measurement of cell dimension is

$$\frac{\Delta (a_1k_1 + a_2k_2)}{(a_1k_1 + a_2k_2)} = \pm \frac{(k_1 + k_2)\Delta a}{(a_1k_1 + a_2k_2)} \pm \frac{(a_1 + a_2)\Delta k}{(a_1k_1 + a_2k_2)}$$

$$= \frac{1.5 \times 10^{-5}}{8.2 \times 10^{-3}} \pm \frac{(1.5 \times 10^{-2}) \times 10^{-2}}{8.2 \times 10^{-3}}$$

$$= 1.46 \times 10^{-3} \pm 1.46 \times 10^{-2} = 1.61\%$$

APPENDIX I

THE GIBBS-DUHEM INTEGRATION

Using the basic Gibbs-Duhem equation:

$$d\ln\gamma_{Ag} = -\frac{N_{Bi}}{N_{Ag}}\, d\ln\gamma_{Bi} \tag{1}$$

and substituting,

$$\ln\gamma_{Bi} = a_{Bi}N_{Ag}^{2}$$

Hence

$$d\ln\gamma_{Ag} = -2a_{Bi}N_{Bi}dN_{Ag} - N_{Ag}N_{Bi}da_{Bi} \tag{2}$$

Integrating the above equation from the solubility limit of silver in bismuth to a lower concentration for a given temperature gives:

$$\int_{N_{Ag}^{*}}^{N_{Ag}} d\ln\gamma_{Ag} = -\int_{N_{Ag}^{*}}^{N_{Ag}} 2a_{Bi}N_{Bi}dN_{Ag} - \int_{N_{Ag}^{*}}^{N_{Ag}} N_{Ag}N_{Bi}da_{Bi}$$

$$= -\int_{N_{Ag}^{*}}^{N_{Ag}} a_{Bi}dN_{Ag} - a_{Bi}N_{Ag}N_{Bi} + a_{Bi}^{*}N_{Bi}^{*}N_{Ag}^{*}$$

Therefore,

$$\ln \frac{\gamma_{Ag}}{\gamma_{Ag}^*} = - \int_{N_{Ag}^*}^{N_{Ag}} \alpha_{Bi} dN_{Ag} - \alpha_{Bi} N_{Ag} N_{Bi} + \alpha_{Bi}^* N_{Bi}^* N_{Ag}^* \qquad (3)$$

If γ_{Ag}^* is independently known, γ_{Ag} at a given composition can be determined by plotting α_{Bi} versus compositions. In the silver-bismuth system, γ_{Ag}^*, activity coefficient of silver at liquidus point relative to the supercooled liquid of silver at a corresponding temperature, is calculated from the available thermodynamic data of silver metal, applying an assumption that silver follows the Raoult's law in the silver rich primary solid solution.

In order to determine the activities of silver in the supercooled region, equation (3) is transformed to be,

$$\int_{N_{Ag}^*}^{N_{Ag}=1} \alpha_{Bi} dN_{Ag} = \ln \gamma_{Ag}^* + \alpha_{Bi}^* N_{Bi}^* N_{Ag}^* \qquad (4)$$

The right hand side of equation (4) can be determined and also the value is equivalent to the area of $1/2\ (\alpha_{Bi}^{\bullet} + \alpha_{Bi}^*)\ N_{Ag}^*$, where $\alpha_{Bi}^{\bullet}$ is the value of alpha function at $N_{Ag} = 1$ (or $N_{Bi} = 0$), if α_{Bi} function is assumed to behave linearly with composition. Thus, α_{Bi} at N_{Bi} can be readily obtained from the above relationship.